Modeling metal ion-humic substances complexation in highly saline conditions

Rémi M Marsac, Nidhu L Banik, Johannes L Lützenkirchen, Charlotte Catrouillet, Christian M Marquardt, Karen H Johannesson

Accepted Manuscript

Modeling metal ion-humic substances complexation in highly saline conditions

Rémi Marsac, Nidhu L. Banik, Johannes Lützenkirchen, Charlotte Catrouillet, Christian M. Marquardt, Karen H. Johannesson

PII: S0883-2927(16)30231-1

DOI: 10.1016/j.apgeochem.2017.02.004

Reference: AG 3821

To appear in: *Applied Geochemistry*

Received Date: 19 August 2016

Revised Date: 23 January 2017

Accepted Date: 1 February 2017

Please cite this article as: Marsac, R., Banik, N.L., Lützenkirchen, J., Catrouillet, C., Marquardt, C.M., Johannesson, K.H., Modeling metal ion-humic substances complexation in highly saline conditions, *Applied Geochemistry* (2017), doi: 10.1016/j.apgeochem.2017.02.004.

Modeling metal ion-humic substances complexation in highly saline conditions

Rémi Marsac[1,2,]*, Nidhu L. Banik[2,3], Johannes Lützenkirchen[2], Charlotte Catrouillet[1], Christian M. Marquardt[2], Karen H. Johannesson[4]

*Corresponding author: e-mail address: remi.marsac@univ-rennes1.fr
Tel: +332 23 23 53 56. Fax: +332 23 23 60 90
[1]Géosciences Rennes UMR 6118, Université Rennes 1, CNRS, 35042 Rennes cedex, France.
[2]Institute for Nuclear Waste Disposal, Karlsruhe Institute of Technology, P.O. Box 3640, D-76021 Karlsruhe, Germany.
[3]JRC-KARLSRUHE, G.II.6 - Nuclear Safeguards and Forensics, European Commission, P.O.Box 2340, D-76125 Karlsruhe
[4]Department of Earth and Environmental Sciences, Tulane University, 6823 St. Charles Avenue, New Orleans, LA 70118, USA.

Highlights:

- Model VII and NICA-Donnan are tested at high ionic strength (*I*) using the SIT.
- For *I* > 1 m, Model VII is applicable as a non-electrostatic model.
- No modification is needed for NICA-Donnan.
- Both models predict the effect of *I* on proton- and metal ion-humate (M-HA) binding.
- SIT parameters for simpler M-HA binding models vary with pH and metal loading.

Abstract. Because highly saline groundwaters are found at potential repository sites for nuclear waste, geochemical models should predict the speciation of relevant radionuclides in brines, including their complexation with substances such as humic acids (HA). In this study, available experimental radionuclide-HA complexation data in high 1:1 background electrolyte solutions ($0.01 < m_{\mathrm{NaCl}/NO_3/\mathrm{ClO}_4} < 4$ molal, *m)* are reviewed. Discrepancies in the amplitude of ionic strength effects on radionuclide-HA complexation are observed, which might depend on the nature of the interacting radionuclide or on the origin of HA. However, significant differences in the experimental conditions and calculations applied to determine conditional metal ion-HA complexation constants hamper direct comparison between these datasets. To clarify whether metal ion-HA binding in saline solutions can be described, two sophisticated humic-ion binding models (Model VII and NICA-Donnan) are presently used. This is the first time that Model VII and NICA-Donnan are applied to predict metal ion-HA binding at high ionic strength (I > 1 m). The advantage of these models, compared to more simple ones (e.g., the polyelectrolyte or the charge neutralization models), is that both electrostatic and chemical contributions to the overall metal ion-HA binding are explicitly taken into account. Model VII and NICA-Donnan are shown to produce very similar results. Trends in conditional metal ion-HA binding constants and in the maximum metal ion uptake by HA (e.g., the loading capacity) with I agree with experiments. The present data evaluation suggests that most of the apparent discrepancies between various experimental datasets arise from differences in the experimental conditions. Both Model VII and NICA-Donnan predict that the specific ion interaction theory (SIT) parameters for metal ion-HA systems, which are required for high ionic strength with more simple models, vary with pH and metal loading. Overall, Model VII and NICA-Donnan are able to account for various mechanisms involved in metal ion-HA complexation, including the metal loading effects and cation

competition, and might be helpful predictive tools for performance safety assessment up to highly saline conditions.

Keywords: humic, radionuclide, complexation, brine, saline, Model VII, NICA-Donnan, specific ion interaction theory.

1. Introduction

Humic substances (HS) such as humic (HA) and fulvic (FA) acids are ubiquitous in natural waters and form complexes with dissolved metal ions. They play a crucial role for metal ion mobility and bioavailability in the environment. HS exhibit extreme complexity. The major HS cation-binding groups are the carboxylic and phenolic groups (Ritchie and Perdue, 2003), but less abundant softer Lewis bases (e.g., N- and S-containing groups) also contribute to cation-HS complexation (Tipping, 1998; Hesterberg et al., 2001). HS are macro-ions and electrostatic effects are relevant for their complexation properties. Moreover, several HS groups may bind a single cation, which either leads to a chelation effect (Martell and Hancock, 1996) or to the formation of a cation bridge between different organic molecules (e.g., Kunhi Mouvenchery et al., 2012). Hence, metal ions can form a large variety of complexes with HS, leading to apparent complexation constants that depend on pH, ionic strength and metal ion/HS concentration ratio (i.e., the metal loading) including the presence of competing cations like Ca and Mg. Substantial efforts have been made to determine thermodynamic metal ion-HS complexation constants and to develop predictive models for environmentally relevant conditions (e.g., Kim and Czerwinski, 1996; Benedetti et al., 1995; Tipping, 1998; Milne et al., 2001; 2003; Sasaki et al., 2008). Because of the complexity of HS, very different approaches have been proposed to describe the reaction between HS and metal ions.

The resulting metal ion-HS complexation models were developed for, and mainly applied to describe metal ion speciation under freshwater conditions, but were shown to be applicable for the more saline conditions that occur in estuaries and seawaters (e.g., Hiemstra and van Riemsdijk, 2006; Turner et al., 2008; Stockdale et al., 2011). Nonetheless, few studies have investigated metal ion-HS interactions under highly saline conditions, such as ionic strength (I) exceeding that of seawater (i.e., $I > 0.7$ m). The latter conditions are relevant with regard to the

safety of nuclear waste disposal in rock salt formationsor in specific clay formations. For example, deep waters in the Jurassic and lower Cretaceaous clay rock formations in Northern Germany may contain salt concentrations as high as about 4 M (Mühlenberg et al., 1997). Sedimentary rocks currently investigated in Canada are in contact with brine solutions up to 6.5 M (Fritz and Frape, 1982). Although high ionic strength commonly leads to the coagulation of HS, this process has been shown to be incomplete in many cases and non-negligible amounts of dissolved HS were reported to persist (Wall and Choppin, 2003), which can react with dissolved metal ions.

Most of the radionuclide-HS complexation studies in saline solutions focused on HA. Because few data for FA exist, only HA binding properties at high ionic strength are discussed herein. Generally, at constant pH, the apparent radionuclide-HA complexation constants in monovalent background electrolyte solutions (e.g., NaCl or $NaClO_4$) decrease with increasing ionic strength from very dilute aqueous solutions up to 1 molal (mol kg^{-1}, hereafter denoted *m*). However, different binding behaviors are observed for $I > 1$ *m*. Specifically, UO_2^{2+}- and Pu^{4+}-HA complexation constants increase with increasing ionic strength (Labonne-Wall et al., 1999; Szabò et al., 2010), whereas Co^{2+}-HA complexation does not vary substantially, and Ni^{2+}-HA complexation slightly decreases (Kurk and Choppin, 2000) with increasing ionic strength. Although data from Czerwinski et al. (1996) and Wall et al. (2002) consistently show increasing Am^{3+}/Cm^{3+}-HA binding with increasing *I*, Czerwinski et al. (1996) observed minor variation in complexation constant values with *I*. This led them to propose an average value (with standard variation of ± 0.14 log units) for the entire range of *I* investigated, which contrasts with Wall et al. (2002) where much larger variations were reported (about 3 log units). Furthermore, for $1 \leq I \leq 3.5$ *m*, the maximum amount of radionuclide that is experimentally found to bind to HA (e.g., the so called loading capacity in the charge neutralization model) was shown to decrease with

increasing *I* for trivalent actinides (Czerwinski et al., 1996), whereas it remained constant in the case of Pu(IV) (Szabò et al., 2010). All these discrepancies might be indicative of conformational changes in saline solutions, which would depend on the nature of the interacting radionuclide as well as on the origin of HA. However, significant differences exist in the experimental conditions and calculations applied to determine conditional metal ion-HA complexation constants between these different studies, which complicates data comparison. Some studies were conducted in non-complexing background electrolyte solutions ($NaClO_4$; Czerwinski et al., 1996; Szabò et al., 2010). High [Cl^-] is environmentally relevant (as opposed to high [ClO_4^-]), but metal ions can bind Cl^-, which may affect the determination of radionuclide-HA complexation constants. Complexation data for UO_2^{2+}- and Am^{3+}-HA binding from Labonne-Wall et al. (1999) and Wall et al. (2002) were obtained in acetate buffers under ambient (air) atmosphere. Like many ligands, acetate and carbonate form aqueous complexes with UO_2^{2+} and Am^{3+} and can compete with HA. Experiments were conducted at different radionuclide-to-HA concentration ratios, which might also affect HA charge and conformation. Finally, pH measurement is non-trivial in saline solutions. More specifically, "constant pH values" can refer to constant proton activity (pH = - log a_{H^+}; Szabò et al., 2010), proton molality (pH_m = - log m_{H^+}; Czerwinski et al., 1996; Labonne-Wall et al., 1999; Wall et al., 2002), or constant experimental values, as read on the pH-meter (pH_{exp}; Kurk and Choppin, 2000; where the pH_{exp}-pH_m relationship is provided). Deviation between pH, pH_m and pH_{exp} as affected by *I* may also hamper comparison between different datasets.

Available radionuclide-HA complexation data have been analyzed using relatively simple models such as the Polyelectrolyte Model (PM; Torres and Choppin, 1984) or the Charge Neutralization Model (CNM; Kim and Czerwinski, 1996). These models can be conveniently included in the speciation codes used for performance safety assessment. Within these models,

binding parameters may vary with pH and *I*. High salt levels require an appropriate treatment of activity coefficients for aqueous species in geochemical models, such as application of specific ion interaction theory (SIT; Ciavatta, 1980). Metal-HA complexation constants can also be extrapolated to $I = 0$ using SIT, when considering HA as a solute. However, due to HA complexity, SIT parameters are no more than adjustable parameters and their values have no clear physical significance according to the original authors (Czerwinski et al., 1996; Szabò et al., 2010). Given the differences in the experimental conditions between previous radionuclide-HA complexation studies and the different calculations applied for the determination of metal-HA complexation constants (e.g., with the CNM or the PM), it is difficult to evaluate how SIT parameters would evolve with changing metal ion concentrations and physico-chemical conditions.

More sophisticated models exist, such as the humic ion binding Model VII (Tipping et al., 2011), or its previous versions (Models V/VI: Tipping and Hurley, 1992; Tipping, 1998), and the NICA-Donnan model (Kinniburgh et al., 1996; Koopal et al., 2005). The description of HA properties relies on several assumptions, and the various models include a more or less detailed description of metal ion-HA interaction. In particular, the electrostatic and chemical contributions to the overall metal ion-HA binding are separated in the models. This is a major advantage for understanding metal ion-HA binding in saline solutions, because ionic strength is expected to more strongly affect electrostatic than chemical binding properties of HA. Unfortunately, as pointed out by Tipping (1998), the electrostatic approach included in Models V/VI/VII is unlikely to be applicable for $I > 1$ m. In contrast, NICA-Donnan equations seem to be applicable in highly saline conditions (up to 2 M), as shown for HA proton titration data (Benedetti et al., 1996), but, to our knowledge, it has never been tested for metal ion-HA complexation data.

In the following, we evaluate the applicability of Model VII and the NICA-Donnan model for saline aqueous solutions, focusing on the concomitant electrostatic approaches. The following analysis involves close inspection of the model equations in conjunction with comparisons of simulated and experimental HA proton titration and radionuclide complexation data. The mechanisms responsible for the effect of ionic strength on cation-HA complexation are also discussed within the context of the assumptions inherent to Model VII and NICA-Donnan. Finally, the impact of the physico-chemical conditions on the experimental determination of SIT parameters for more simple cation-HA models is discussed.

2. Theoretical background

2.1. Aqueous speciation calculations and codes

Ionic strength (I) affects the activity of dissolved ions in solution, which must be accounted for, for instance, when extrapolating formation constants to hypothetical infinite dilution condition (i.e., for I = 0 m). In the present study, activity coefficients (γ) are calculated according to the specific ion interaction theory (SIT; Ciavatta, 1980). SIT is generally considered valid for ionic strengths up to 3 - 4 m. At 25 °C, activity coefficients for an aqueous species i with a charge z_i are calculated as follows:

$$\log \gamma_i = -{z_i}^2 \frac{0.509 \times \sqrt{I}}{1 + 1.5\sqrt{I}} + \sum_k \varepsilon(i,k) \times m_k = -{z_i}^2 D + \sum_k \varepsilon(i,k) \times m_k \qquad (1)$$

where D is the Debye-Hückel term used in SIT, m_k is the molality of the aqueous species k (mol kg^{-1}), and ε(i,k) is the specific ion interaction coefficient between species i and k (kg mol^{-1}).

In the present study, we use PHREEQC (version 2; Parkhurst and Appelo, 1999) to model cation-HA binding with Model VII. The NICA-Donnan model is not implemented in PHREEQC yet, which will require future modification of PHREEQC code. Therefore, Visual MINTEQ

(version 3.0; Gustafsson, 2012) is used to model cation-HA binding with NICA-Donnan. The SIT database provided with each code is used (which corresponds to ThermoChimie v.7.b in PHREEQC). Unless mentioned in this study, the same thermodynamic constants and SIT parameters were selected throughout. The metastability of ClO_4^-, sometimes used as background anion, is avoided in the models by defining perchlorate as a master species. The Pitzer approach (Pitzer, 1991) can be applied to calculate activity coefficients for aqueous ions in even more concentrated media than appropriate for SIT, which would be more relevant for brine solutions. However, in the present study, the SIT was chosen: (i) for the sake of simplicity, as it is approximately equivalent to a simplified Pitzer model (Grenthe et al., 1993); (ii) because most of the thermodynamic data are taken from the NEA database (Guillaumont et al., 2003), which recommends the use of SIT; and (iii) because Pitzer equations are implemented in PHREEQC but not in Visual MINTEQ, the NICA-Donnan model cannot be tested yet in combination with the Pitzer model.

Experimental pH measurements (pH_{exp}) are affected by the background electrolyte concentration under saline conditions (e.g., Altmaier et al., 2003), and appropriate calibrations are necessary to relate empirical pH_{exp} to the molality of the proton ($pH_m = -\log m_{H^+}$). The deviation between pH_{exp} and pH_m increases with increasing ionic strength such that $pH_{exp} < pH_m$ for concentrated electrolytes. The pH ($= -\log a_{H^+}$), which is a master variable and hence required by speciation codes, can be determined from pH_m and calculated γ_{H^+} values. In this study, SIT is used to calculate pH.

2.2. Determination of empirical metal ion-HA complexation constants

Empirical models consider that the metal ion binds to one generic HA site. Non-specific metal ion-HA interactions are not considered explicitly. The general complexation reaction of a cation M with HA can be written as follows:

$$M + HA \ = \ MHA \qquad (2)$$

and the corresponding conditional stability constant is

$$^{HA}\beta = \frac{[MHA]}{[M]_f[HA]_f} \qquad (3)$$

Various approaches can be found in the literature to determine $^{HA}\beta$ values. Therefore, it is not possible to directly compare $^{HA}\beta$ values reported in separate M-HA complexation studies unless the same calculations were made or appropriate corrections are applied. The differences arise from the various possibilities for defining $[M]_f$ or $[HA]_f$ in eq. 3. For example, $[M]_f$ may refer to (i) the total dissolved metal ion concentration at equilibrium (noted $[M]_{tot,f}$ in the following), which includes complexes of M with any ligand except HA (e.g. OH^-, Cl^-, CO_3^{2-} or acetate when used as a pH buffer) or (ii) the "free" aquo-ion only, $[M^{z+}]_f$. In the remainder of the text, M-HA complexation constants referring to the total dissolved metal ion concentration and to the aquo-ion will be denoted $^{HA}\beta(M)$ and $^{HA}\beta(M^{z+})$, respectively. $[M^{z+}]_f$ can be calculated by dividing the $[M]_{tot,f}$ value by the side reaction coefficient (α_M; Ringböm, 1963):

$$\alpha_M = 1 + \sum_h \frac{^*\beta_h}{m_{H^+}^h} + \sum_l \beta_l \times m_L^l \ . \qquad (4)$$

Here, $^*\beta_h$ are the hydrolysis constants, L is a ligand, β_l are the formation constants for $M(L)_l$ complexes and m_{H^+} and m_L refer to the molalities of H^+ and L. In eq. 4, $^*\beta_h$ and β_l are conditional constants, valid at a given ionic strength. Possible ternary complexes (i.e., involving a

metal ion and two different ligands) or polynuclear species are not included in eq. 4 for the sake of simplicity in the present text, but they must be taken into account in the calculations.

The definition of $[HA]_f$ (eq. 3) also depends on the humic-ion binding model considered. In the present study, the notation of Marquardt and Kim (1998) is used for the different ${}^{HA}\beta$ (namely, ${}^{HA}K$, ${}^{HA}\beta_{LC}$ or ${}^{HA}\beta_{\alpha}$, as defined below). HA site density, commonly corresponding to the proton exchange capacity of HA (PEC, in eq $g(HA)^{-1}$), can be taken into account to determine the total HA site concentration ($[HA]_{tot}$, in eq $kg(H_2O)^{-1}$). The corresponding M-HA complexation constant, denoted ${}^{HA}K$, can be calculated considering that:

$$[HA]_f = [HA]_{tot} - [MHA] \quad (5)$$

where ${}^{HA}K$ varies with pH, ionic strength, metal loading, etc.

Competition between the metal ion and H^+ can be included via the degree of deprotonation (α_{HA}) in order to suppress the dependence of the M-HA complexation constant on pH:

$$[HA]_f = [HA]_{tot} \times \alpha_{HA} - [MHA]. \quad (6)$$

The concomitant complexation constant is noted ${}^{HA}\beta_{\alpha}$ and refers to the Polyelectrolyte Model (PM; Torres and Choppin, 1984). The degree of deprotonation, α_{HA}, is experimentally determined by proton titration and depends on both pH and ionic strength.

Another approach is to consider the effective amount of binding sites at a given pH and *I*. Here, the aim is to suppress the dependence of the M-HA complexation constant on both pH and HA site saturation at high metal loading. In a Pu(IV)-HA study, Szabó et al. (2010) determined the maximum complexing capacity (B_{max}, in mol g^{-1}) of HA immobilized on silica gel (19.9 mg HA g^{-1}), associated with a complexation constant denoted ${}^{HA}\beta(Pu^{4+})$:

$$[HA]_f = B_{max} - [PuHA] \quad (7)$$

where B_{max} and ${}^{HA}\beta(Pu^{4+})$ are determined by analyzing SiO_2-HA-Pu binding isotherms with a Langmuir-type equation.

The effective amount of binding considered in the Charge Neutralization Model (CNM; Kim and Czerwinski, 1996) is the "loading capacity" (LC, generally in mol g^{-1}). For this model, it is assumed that the total amount of HA sites that is available to neutralize the metal depends on the metal charge (z). In the CNM, the free HA site concentration is defined as:

$$[HA]_f = [HA]_{tot} \times LC/z - [MHA]. \quad (8)$$

The corresponding M-HA complexation constant is noted ${}^{HA}\beta_{LC}$.

2.3. Humic-ion binding models NICA-Donnan and Model VII

2.3.1. Chemical part of the models

NICA-Donnan and Model VII have been described in several publications (e.g., Koopal et al., 2005; Tipping et al. 2011). Because the effect of the ionic strength is taken into account through the electrostatic part of these models, the chemical part is only briefly discussed here. Cation-HA complexation (including H^+) in NICA-Donnan and Model VII follows identical reaction equations (eq. 2). Additional equations are used to account for HA heterogeneity. NICA-Donnan describes HA heterogeneity by a continuous affinity distribution for the interaction between a cation and HA, whereas Model VII considers a large number of binding sites with different but discrete affinities for the cation. The chemical cation-HA binding parts of these models aim at describing the overall cation-HA complexation (e.g., expressed as a log ${}^{HA}K$ value) as a function of pH, cation to HA concentration ratio (or "metal loading"), and take into account cation competition with a limited number of parameters. The latter parameters are "intrinsic" because they do not vary with the physico-chemical conditions. However, parameters usually vary with the type of HA, including origin or composition. Generic parameters for a wide range

of metal ions and HAs were determined for NICA-Donnan (Milne et al., 2001; 2003) and Model VII (Tipping et al., 2011) by fitting experimental datasets. These generic parameters capture "average" HA behavior, and will be used as such in this study. Consequently, the present work does not aim at discussing the capability of the generic parameters to precisely simulate a given dataset (i.e., no parameter optimization is made). Rather the capability of NICA-Donnan and Model VII to predict variations in apparent cation-HA binding constants with the ionic strength will be discussed (e.g., trends in log ^{HA}K versus I).

It is important to note that, in NICA-Donnan and Model VII, Na^+ is not considered to bind specifically to HA unlike Ca^{2+} or Mg^{2+}, which complex with HA in solution. Therefore, for high 1:1 Na-containing background electrolyte solution (e.g. $NaCl/NO_3/ClO_4$), Na^+ is considered to control the ionic strength and to affect other metal ion complexation by HA only via electrostatic effects.

2.3.2. Electrostatic models

HAs are large and negatively charged polyelectrolytes. This leads to an accumulation of cations in the vicinity of HA binding sites. Electrostatic models aim at converting the dissolved cation concentration in the bulk solution ($[C]_i$) to a local dissolved cation concentration ($[C]_{loc,i}$) that occurs adjacent to the HA site. To accomplish this, the electrostatic potential of HA particles (Ψ, in V) is computed using a Boltzmann factor:

$$[C]_{loc,i} = [C]_i \times \exp(-z_i F\Psi/RT) \quad (9)$$

Here, z_i is the charge of the cation, T is absolute temperature, F is the Faraday constant and R is the gas constant.

Within the NICA-Donnan framework, HAs are considered as permeable spheres. Counter-ions are accumulated in a Donnan phase. The electrostatic potential (Ψ_D) is constant

inside the Donnan volume and equals zero outside (i.e., in the bulk solution). The Donnan volume (V_D, in L kg(HA)$^{-1}$) is calculated as follows:

$$\log V_D = b(1 - \log I) - 1 \quad (10)$$

The parameter b is adjusted by fitting acid-base titration experiments at varying I and depends on the type of HA (origin, composition, etc). In the Donnan volume, the negative charge of HA (Q) is neutralized by counterions:

$$\frac{Q}{V_D} + \sum_i z_i \left([C]_{D,i} - [C]_i\right) = 0 \quad (11)$$

where $C_{D,i}$ and C_i refer to the concentration of the ion i with a charge z_i in the Donnan phase and in the bulk solution, respectively. The activity of the ion in the Donnan phase is required for calculation of the specific binding.

Within the Model VII framework, HA molecules are considered as impermeable spheres. Since the conceptualization of HA particles and the numerical treatment of the electrostatic effects resemble a surface complexation model (e.g., see the present implementation of Model VII in PHREEQC in the following section), we will denote the electrostatic potential Ψ_0, similarly to the surface potential of minerals. The electrostatic correction is an empirical equation that mimics the Boltzmann factor:

$$\exp(-F\Psi_0/(RT)) = \exp(-2PQlog(I)) \quad (12)$$

where I is the ionic strength (mol L^{-1}), P is an adjustable parameter (generally -400 < P < -100 for HA) and Q is the net humic acid charge (eq g^{-1}). In NaCl/NO_3/ClO_4 background electrolytes, the molality and molarity scales do not significantly differ for $I \leq 1$ M (or m). The molality scale is used to extrapolate the model to high I. A Donnan model is also used in the original version of Model VII, but it only accounts for counter-ion accumulation (i.e., to calculate the amount of ion bound to HA in a non-specific manner) and has no effect on electrostatics, in contrast to the NICA-Donnan model. Because in Model VII, HA is considered to be an impermeable sphere of

radius r, the Donnan volume is a layer at the surface of the sphere, with a thickness equal to the Debye length ($\kappa^{-1} = (3.29\times10^{9}\times I^{1/2})^{-1}$; in meters, I in mol L^{-1} and at 25°C). With the molar mass and the radius of HA (15000 g mol^{-1}; 1.72 nm) inherent to Model VII, the surface area of HA (A_{HA}) equals 1500 m^2 g^{-1}. Hence, the Donnan volume in Model VII equals $A_{HA}\times\kappa^{-1}$ (in m^3 g^{-1}). Unfortunately, the "-donnan" keyword cannot be used with SIT and Pitzer options in PHREEQC. It can only be used with other databases, which do not involve SIT or Pitzer models (e.g. which use Davies or Debye-Hückel equations to calculate activity coefficients). However, during preliminary tests, we found very little effect of these calculations on the overall cation-HA binding (see Fig. S2), especially at high I where the Donnan volume drastically shrinks. Therefore, this option is not used in the present study, that is, counter-ion accumulation is neglected.

2.3.3. Implementation of Model VII in PHREEQC

The complete Model VII chemical reaction database, described in Tipping et al. (2011), was previously included in PHREEQC by Marsac et al. (2014) and is used in this study. In the supporting information, a file that can be used to modify Model VII chemical reaction database (e.g., to include other cations or to change binding parameters) and an example of PHREEC input file are given.

Previous studies, where Models V, VI or VII were coupled with PHREEQC, attempted to convert this empirical electrostatic humic ion-binding model into the diffuse layer model (DLM) formalism (Appelo and Postma, 2005; Liu et al., 2008; Marsac et al., 2011, 2014; Catrouillet et al., 2014). Such a conversion requires the calculation of a surface area (A_{HA}) that depends on the ionic strength. Similar computations have been performed for polyelectrolytes such as polyacrylic acid (Lützenkirchen et al., 2011). Such approaches result in physically unreasonable

surface areas (above 10^4 m² g^{-1}) (Appelo and Postma, 2005; Liu et al., 2008; Lützenkirchen et al., 2011; Marsac et al., 2011, 2014; Catrouillet et al., 2014). Hence, we suggest the use of the constant capacitance model (CCM) might be a better choice (Catrouillet et al., 2015). For the CCM, the capacitance (C_1, in F m^{-2}) evolves with log *I* in the case of minerals (Lützenkirchen, 1999), and a log *I*-term is also found in the empirical electrostatic model in Model VII (eq. 12). Specifically, the CCM employs a linear relationship between the charge density at the surface (σ_0, in C m^{-2}) and the surface potential (Ψ_0, in V):

$$\sigma_0 = C_1 \times \Psi_0. \quad (13)$$

Combination of equations 12 and 13 gives:

$$C_1 = F^2 \times (2RTPA_{HA}\log(I))^{-1}. \quad (14)$$

Therefore, using the CCM leads to an expression for C_1 that does not depend on the pH. Given the surface area of HA in Model VII (A_{HA} = 1500 m² g^{-1}), the range of C_1 values found for $I < 1$ *m* corresponds to that commonly reported for minerals ($0.5 < C_1 < 10$ F m^{-2}; Lützenkirchen, 1999). Although the CCM is not implemented in PHREEQC, it can be used by applying appropriate corrections to the three plane model (TPM) in PHREEQC. Details are given in supporting information.

3. Results and Discussion

3.1. Proton titration in saline solutions

Although proton titrations of HA are rarely carried out for $I > 1$ *m*, a number of critical studies do exist. Kurk and Choppin (2000) and Laszak and Choppin (2001) performed proton titrations of HA at I = 0.1, 0.3, 1, 3 and 5 *m* (NaCl), and calculated apparent dissociation constants (pK_a) for HA considering two acidic groups. They found that pK_a variation was insignificant (±0.1) within this range of ionic strengths. Marinsky et al. (1982) reported similar

observations for ionic strength between 0.2 and 2 M $NaNO_3$. Furthermore, the charging curves for HA versus the pH_m reported by Maes et al. (1992) exhibited only slight differences between 1 and 3 M $NaClO_4$. Van Dijk (1959) observed a shift in the titration curves to lower "pH" for *I* increasing from 0.02 to 2 M NaCl but mentioned no pH-correction. This effect is qualitatively consistent with the increased deviation between pH_{exp}-pH_m with increasing *I* ($pH_{exp} < pH_m$) that is commonly observed (e.g., Kurk and Choppin, 2000; Altmaier et al., 2003). The surface of biological cells, such as the seaweed *Ulva lattuca*, can be considered as a polyelectrolyte, and the cation sorption properties onto *U. lattuca* can be treated with the models applied to HA (e.g. Turner et al., 2008). Surface acid-base properties of such biosorbents show very little influence of *I* above 1 *m* (e.g. Rey-Castro et al., 2003; Schijf and Ebling, 2010).

The apparent pK_a of one HA site at a given ionic strength ($pK_a(I)$), which is obtained experimentally, can be written as follows:

$$pK_a(I) = -log\frac{[H^+][HA^-]}{[HHA]} = pK_a(I=0) + log\,(\gamma_{H^+}) - F\Psi/(RTln(10)) \qquad (15)$$

According to eq. 15, the observed small dependence of conditional HA proton dissociation constants on *I* for highly saline conditions (*I* > 1 *m*) might occur (i) due to small dependencies of both Ψ and γ_{H^+}on *I* or (ii) compensation of the effects of *I* on Ψ and γ_{H^+}. Figure 1a compares the effect of *I* on Ψ_0 (for Model VII) and Ψ_D (for NICA-Donnan) at constant proton activity (pH = 5.5). As stated by Tipping (1998), Model VI is unlikely to find application at ionic strengths higher than *I* = 1 *m*, because of the electrostatic model (the same is true for Model VII). When the electrostatic term is translated to the CCM formalism (e.g., to be used in PHREEQC; eq. 14), and for the case when *I* increases to 1 *m*, C_1 tends to infinity and the model becomes essentially non-electrostatic (Ψ_0 = 0). When *I* > 1 *m*, C_1 is negative, which is physically unrealistic,

demonstrating that Model VII cannot be used with PHREEQC when $I > 1$ *m* (except by suppressing the electrostatic term), consistent with the conclusion of Tipping (1998).

Benedetti et al. (1996) previously demonstrated the capability of NICA-Donnan to simulate HA charging curves versus pH in highly saline conditions (up to 2 M). In this case Ψ_D increases with I and only small variation in Ψ_D can be seen for $I > 1$ *m* (Fig. 1a). The NICA-Donnan model's inherent electrostatic contribution in cation-HA binding is approximately constant (-60 mV $\leq \Psi_D \leq$ -40 mV) for $I > 1$ *m*, and only a small dependence of apparent pK_a values (i.e., corrected for the activity coefficient effect) on Ψ_D is predicted. This is because the Donnan volume is small for $I > 1$ *m* and only slightly shrinks when I further increases. Interestingly, the amplitude of the variation in Ψ is similar for both models when using the generic parameters: $\Psi_D \approx \Psi_0 - 60$ mV for $I < 1$ *m* and pH = 5.5, as highlighted in Figure 1a. Therefore, by suppressing the electrostatics in Model VII for $I \geq 1$ *m*, we produce a comparable effect of I on cation-HA binding constants as in NICA-Donnan. This leads to a simplification of Model VII equations compared to lower I.

Figure 1b shows the change of $\log \gamma_{H^+}$ versus I between 0.1 and 4 *m* for different background electrolyte solutions (i.e., $NaNO_3$, NaCl, and $NaClO_4$) computed according to the SIT equation, where $\varepsilon(H^+,NO_3^-) = 0.07 \pm 0.07$ for $NaNO_3$, $\varepsilon(H^+,Cl^-) = 0.12 \pm 0.01$ for NaCl, and $\varepsilon(H^+,ClO_4^-) = 0.14 \pm 0.03$ for $NaClO_4$ electrolytes. The maximum variation in $\log(\gamma_{H^+})$ between 1 and 4 *m*, as calculated with SIT, is approximately 0.16 in $NaNO_3$, 0.31 in NaCl and 0.37 in $NaClO_4$, corresponding to a small dependence of the predicted apparent pK_a values on $\log(\gamma_{H^+})$. The slight variation in both Ψ and γ_{H^+} for $1 < I < 4$ *m* is consistent with the experimental observations showing little dependence of apparent pK_a with I under highly saline conditions (Marinsky et al., 1982; Maes et al., 1992; Kurk and Choppin, 2000). Note that the value of γ_{H^+} has no direct impact on NICA-Donnan results, because concentrations are involved in the

equations, and cannot compensate the effects of I on Ψ_D. Therefore, a slight decrease in $pK_a(I)$ values is predicted with the NICA-Donnan Model when I increases.

To illustrate how PHREEQC-Model VII reproduces acid-base titration data for I > 1 m, Figure 1c shows HA charge versus pH_m in 0.1, 1 and 3 M (0.1, 1.051, 3.503 m) $NaClO_4$ determined by Maes et al. (1992), together with results from Model VII. Experimental data of Marinsky et al. (1982) (in $NaNO_3$) and Laszak and Choppin (2001) (in NaCl) with Model VII simulations are shown in Figure S4. For a better illustration, slight adjustment of site densities and pK_a values was made (see table S1), in order to better reproduce experimental data for I = 0.1 M, and predictions are made for higher I. HA charge increases between I = 0.1 and 1 M, which is well predicted. Between I = 1 and 3 M, experimental HA charge decreases, as also predicted by Model VII. This charge decrease is actually related to the use of a pH_m-scale: with a pH-scale (see Fig. S3), Model VII simulations for I = 1 and 3 M cannot be differentiated (due to the suppression of the electrostatic term), and the difference between the two experimental curves is smaller. Beside small discrepancies between experimental and model results, it can be concluded that Model VII does a relatively good job in predicting HA charging curves in saline conditions.

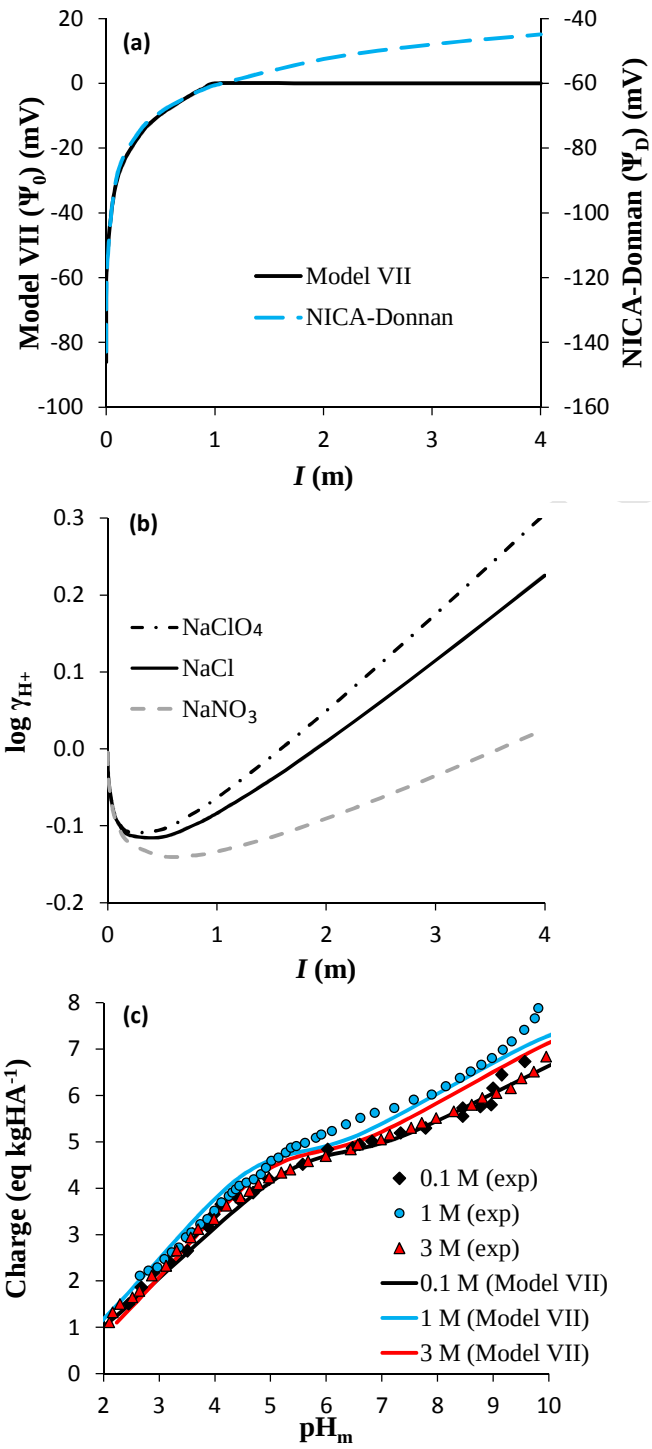

Figure 1. (a) Surface potential (Ψ_0) and Donnan potential (Ψ_D) calculated for Model VII and NICA-Donnan, respectively, for pH (= - log a_{H^+}) = 5.5 versus the ionic strength. The y-axis for Ψ_D is shifted by 60 mV compared with the one of Ψ_0 to highlight their similar evolution with *I*. (b) Activity coefficient of the proton (log γ_{H^+}) versus *I* in NaCl, $NaClO_4$ and $NaNO_3$ solutions,

calculated with SIT. (c) HA charge versus pH_m in 0.1 M (black curve), 1 M (blue curve), and 3 M (red curve) [0.1, 1.051, 3.503 m, respectively] $NaClO_4$. Points are experimental results of Maes et al. (1992) and lines are results from Model VII. (For interpretation to references to color, the reader is referred to the web version of this article.)

3.2. Anticipated effects of high ionic strengths on metal ion-HA binding

As for the proton, apparent metal ion complexation constants with one HA site at a given ionic strength (log K(I); data that can be obtained experimentally) can be calculated as follows:

$$\log {}^{HA}\beta\,(I) = log\frac{[MHA^{z_i-x}]}{[M^{z_i+}][HA^{x-}]}$$

$$= \log {}^{HA}\beta\,(I=0) + log\,(\gamma_{M^{z_i+}}) - z_i F\Psi/(RTln(10)) \qquad (16)$$

The term $z_i F\Psi/(RTln(10))$ leads to substantial log ${}^{HA}\beta$(I) variations for $I < 1\ m$. The amplitude of log ${}^{HA}\beta$(I) variations should increase with increasing metal ion charge z_i. It should also vary with Ψ, and hence with the HA charge, Q. Therefore, we can expect that larger log ${}^{HA}\beta$(I) variations would be observed at high pH and low metal loading compared to low pH and high metal loading. These three anticipated effects are purely related to HA physico-chemical behavior, which are predicted by Model VII and NICA-Donnan equations and parameters.

Other effects can be anticipated, which are not related to HA behavior but to physico-chemical phenomena in solution. As for the proton, $\gamma_{M^{z_i+}}$varies with the ionic strength and the nature of background electrolytes (eq.1), which would directly affect log ${}^{HA}\beta$(I) in eq.16. In the presence of complexing ligands other than HA (e.g., OH^-, CO_3^{2-}, Cl^-, acetate, etc), conditional metal-ligand complexation constants will also evolve with ionic strength, which would affect α_M(eq.4). Therefore, we can expect that (i) the presence of ligands will affect trends in log ${}^{HA}\beta$ versus I whatever the mathematical expression used for log ${}^{HA}\beta$ (see section 2.2) is, and (ii) M-HA complexation constants referring to the total dissolved metal ion concentration (${}^{HA}\beta$(M)) and

to the aquo-ion ($^{HA}\beta(M^{z+})$) might diverge when varying *I*. For instance, if all conditional metal-ligand complexation constants increase with increasing *I*, $^{HA}\beta(M)$ will decrease, whereas $^{HA}\beta(M^{z+})$ will increase because α_M increases with increasing *I*. Prediction of ionic strength effects on $\gamma_{M^{z_i+}}$ and metal-ligand complexation constants pertain to the thermodynamic database used for aqueous solution (thermodynamic constants and SIT parameters). Therefore, in the presence of ligands other than HA, it is more difficult to test the applicability of Model VII and NICA-Donnan in saline solutions because ionic strength effects on metal-ligand complexation must be discussed in parallel. In particular, experiments conducted in NaCl solutions are affected by M-Cl complexation, which increases with increasing [Cl^-], and consequently, the conditional M-Cl complexation constants also evolve with *I*. For this reason, metal ion-HA binding data measured in $NaClO_4$ are initially discussed below (i.e., section 3.3), followed by data collected in NaCl background electrolyte solutions (section 3.4).

3.3. Cation-HA complexation in $NaClO_4$ solutions

Am(III)/Cm(III). Czerwinski et al. (1996) investigated Am^{3+} and Cm^{3+} complexation with HA at pH_m = 6 and in various *I* ($NaClO_4$ electrolyte solution). Because (i) most of the data are available for Am^{3+} and (ii) Am^{3+} and Cm^{3+} are generally considered as chemical analogues, they will not be distinguished and we will only refer to Am^{3+} for both datasets in this section. The authors interpreted the data according to the CNM. Only those datasets that allow the determination of the *LC* (i.e., for *I* = 0.01, 0.1, 1.05 and 3.5 *m*) and that are within the applicability of SIT (*I* < 4 *m*) are considered in the present study. The original authors provided the complete raw dataset, which are not reproduced herein. The data are plotted in the form of a binding isotherm, [AmHA] (in mol kg_{HA}^{-1}) versus $[Am]_{tot,f}$ (in μm), for each *I* on Figure 2a. Note that the experimental data for $[Am]_{tot,f}$ > 8 μm, which are only available for 0.1 and 3.5 *m*, are not

shown for clarity. In addition, the two separate series of experiments in I = 0.01, 0.1 and 1 m cannot be visually distinguished on Figure 2a. All the isotherms exhibit a plateau at ~1 mol kg_{HA}^{-1}. However, a linear decrease of the LC was observed with $\sqrt{I}$. For I < 1 m, log ${}^{HA}\beta_{LC}$ was shown to decrease, whereas it increased for I > 1 m, although in all cases the maximum variation in log ${}^{HA}\beta_{LC}$ is relatively small. Accordingly, the original authors reported an average value of log ${}^{HA}\beta_{LC}$ = 6.24 ± 0.14. Below, we test the capabilities of Model VII and NICA-Donnan to predict the effect of the ionic strength on log ${}^{HA}\beta_{LC}$ and LC for data from Czerwinski et al. (1996). To do so, simulations are made with Model VII and NICA-Donnan under the same conditions as those studied by Czerwinski et al. (1996). The model results are then treated using the equations of the CNM.

The results of the simulations with Model VII are shown on Figure 2a, where the measured and simulated Am-HA binding isotherms for various I are compared. Some discrepancies (either underestimation or overestimation of the model) are observed, which we attribute to the use of generic Model VII parameters and will not be further discussed. As observed experimentally, Model VII predicts decreasing Am-HA complexation with increasing I from 0.01 to 1 m. However, unlike the experimental results, Am-HA complexation is predicted to increase as ionic strength increases from 1 m to 3.5 m $NaClO_4$. Because Model VII is used as a non-electrostatic model (Ψ_0 = 0) for $I \geq 1$ m, the discrepancy between the experimental data and the model results can best be explained by changes in the activity coefficient of Am^{3+}, which increases between 1 and 3.5 m $NaClO_4$ according to SIT ($\varepsilon(Am^{3+},ClO_4^-)$ = 0.49 kg mol^{-1}; Guillaumont et al., 2003), as anticipated in eq.1 and eq.16.

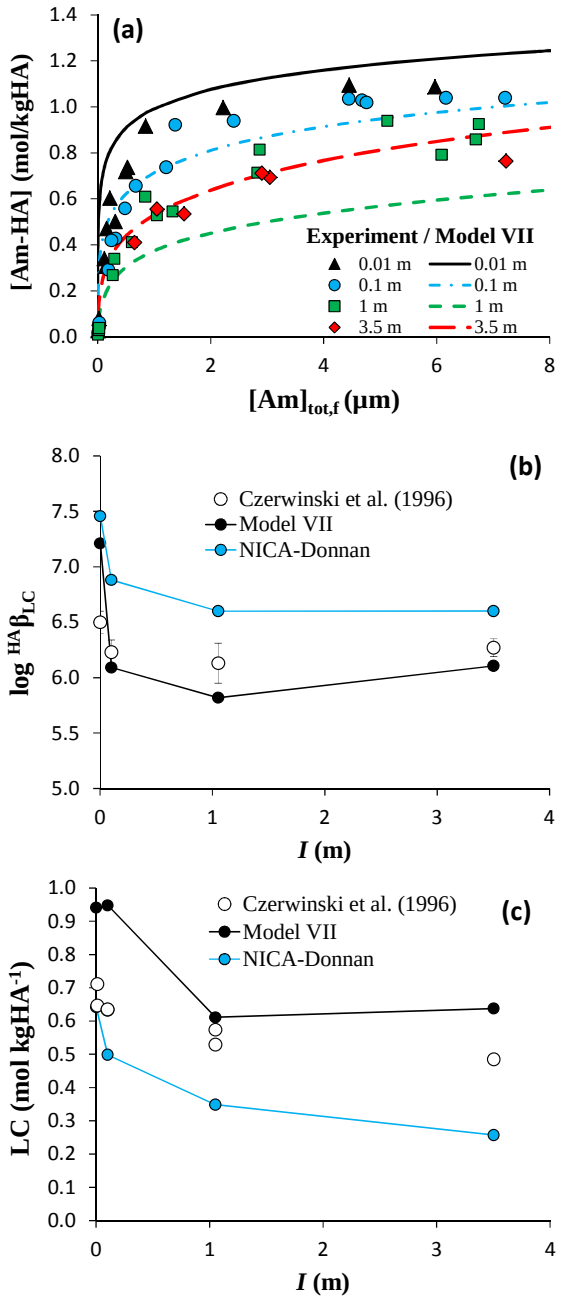

Figure 2. (a) Experimental Am-HA binding isotherms of Czerwinski et al. (1996) for pH_m = 6 and m_{NaClO_4} = 0.01, 0.1, 1 and 3.5 m (symbols) compared with simulations using Model VII (lines). Experimental (b) log $^{HA}\beta_{LC}$ and (c) loading capacity (*LC*) values for Am compared with Model VII and NICA-Donnan predictions versus *I* ($NaClO_4$) in the experimental conditions of Czerwinski et al. (1996). Experimental error bars are generally smaller than the symbols.

Although Model VII accounts for HA heterogeneity, over a limited range of $[Am]_{tot}$, the model Am-HA isotherm can be approximated by a Langmuir-type isotherm. With this approximation, simulations of Am-HA binding with Model VII are treated according to the CNM equations (given in detail in Czerwinski et al., 1996) to determine ${}^{HA}\beta_{LC}$ and *LC*. The results are plotted, respectively, on Figure 2b and 2c. Within the CNM formalism, Model VII consistently predicts a decrease of both *LC* and ${}^{HA}\beta_{LC}$ with increasing *I* from 0.01 and 1 *m*. The increasing activity of Am^{3+} between 1 and 3.5 *m* $NaClO_4$ leads to an apparent increase of both *LC* and ${}^{HA}\beta_{LC}$. Overall, the effect of *I* predicted by Model VII is consistent with the experimental observations although the variations in *LC* and ${}^{HA}\beta_{LC}$ values are larger, as already pointed out. The same exercise with NICA-Donnan yields *LC* and ${}^{HA}\beta_{LC}$ that are also shown in Fig. 2b,c. Although *LC* and ${}^{HA}\beta_{LC}$ values obtained with NICA-Donnan are lower and higher than the experimental values, respectively, the effect of *I* is generally well predicted. Unlike Model VII, NICA-Donnan predicts decreasing Am-HA complexation between 1 and 3.5 *m* $NaClO_4$ because the change in $\gamma_{Am^{3+}}$ cannot compensate for the increase in Ψ_D with increasing *I*, according to NICA-Donnan equations (i.e. based on Am^{3+} concentrations).

Pu(IV). A further example that can be analyzed in the present context is the study by Szabò et al. (2010) on Pu(IV) complexation to a HA grafted silica gel (HA = 20 mg g^{-1}) at pH = 4 and $0.02 < I < 3.5$ *m* ($NaClO_4$). To our knowledge, no Pu(IV)-HA binding parameters are available for NICA-Donnan, and hence, only Model VII can be discussed. The Pu(IV)-HA binding parameters for Model VII are taken from Marsac et al. (2014). Preliminary calculations showed that the formation of polynuclear Pu(IV) species in the presence of HA (Marsac et al., 2014) is not expected for the experimental conditions studied by Szabò et al. (2010). Marsac et al. (2014) used a DLM to account for electrostatic effects when coupling PHREEQC and Model VII,

but the surface area of HA was adjusted to obtain results similar to the original version of Model VII. Here, the same results are obtained when using the CCM to account for electrostatic effects. A modeling approach similar to that used for Am is applied to Pu (Fig. 3). Simulations were performed with Model VII for conditions comparable to those studied by Szabò et al. (2010). The simulated Pu-HA binding isotherms for each ionic strength are treated according to the equations given in the latter study to determine the maximal binding capacity of the HA grafted silica gel for Pu (B_{max}) and log ${}^{HA}\beta(Pu^{4+})$. The calculations include the side reaction coefficient for Pu(IV) (i.e., eq. 4), and the Pu(IV) hydrolysis constants and SIT parameters employed by Szabò et al. (2010), which were originally obtained from Guillaumont et al. (2003). It is important to note that Pu(IV) exhibits strong hydrolysis and that, at pH = 4, α_{Pu} varies with I because of ionic strength effects on conditional Pu(IV) hydrolysis constants.

Simulations with Model VII are compared to the experimental results of Szabò et al. (2010) in Figure 3. The experimental B_{max} decreases with increasing I up to I = 0.5 m and thereafter remains nearly constant up to I = 3.5 m. Model VII predicts little variation in B_{max} with ionic strength (i.e., predicted B_{max} ranges between 0.52-0.59 µmol g^{-1}), in contrast to variation of the experimental results (0.16-1.57 µmol g^{-1}), and to the modeled $LC_{Am(III)}$ variations. Differences between modeling results for Am^{3+} and Pu^{4+} likely arise either from the different metal loadings investigated ([Am(III)-HA] ≤ 1 and [Pu(IV)-HA] ≤ 3×10^{-2} mol $kgHA^{-1}$), which has an impact on HA charge, because Pu^{4+} and Am^{3+} show different hydrolysis behavior, or because HA grafted silica gel behaves differently than dissolved HA. Presently, we cannot explain the discrepancies between experimental and model results for Pu^{4+}. Nevertheless, the predicted variation in B_{max} falls within the experimental range reported by Szabò et al. (2010) so that the impact on the prediction of overall Pu^{4+}-HA binding is limited. Experimental and simulated log ${}^{HA}\beta(Pu^{4+})$ values are also shown in Figure 3. Generally good agreement is found between the experimental

and predicted log $^{HA}\beta(Pu^{4+})$ values (Fig. 3), i.e., a decrease up to I = 1 m followed by an increase up to 3.5 m. The differences are about ±0.5 log units for the stability constant. For Ψ_0 = 0 (i.e., for I > 1 m), the increase in log $^{HA}\beta(Pu^{4+})$ between I = 1 and 3.5 m is due to α_{Pu}, which increases by 0.84 log units over this range of I at pH = 4. Indeed, according to the SIT model, $[Pu^{4+}]$ decreases with increasing I because of the formation of its hydrolysis products (i.e. the $\sum_h \frac{^*\beta_h}{m_{H^+}^h}$ term increases in eq. 4). This phenomenon is not observed with Am^{3+} because its hydrolysis can be neglected at pH = 6 and 0 < I < 4 m.

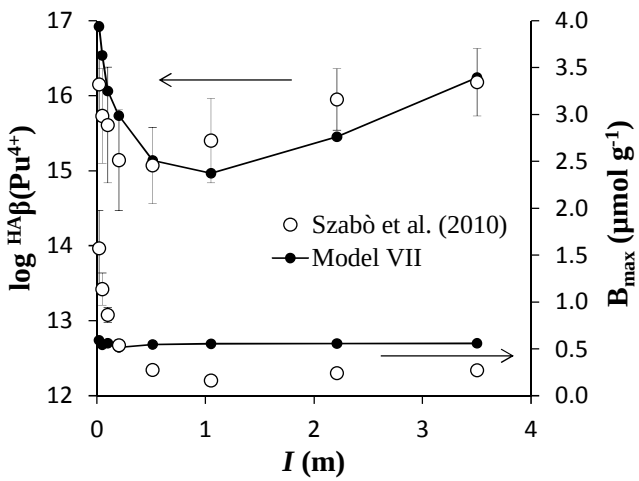

Figure 3. Experimental binding capacity (B_{max}) and log $^{HA}\beta(Pu^{4+})$ values of Szabò et al. (2010) versus I ($NaClO_4$) compared with Model VII predictions. Arrows refer to the y-axis corresponding to the data. Experimental error bars for B_{max} are generally smaller than the symbols.

3.4. Cation-HA complexation in NaCl solutions

In a number of laboratory studies, Choppin and co-workers (Labonne-Wall et al., 1999; Kurk and Choppin, 2000; Laszak and Choppin, 2001; Wall et al., 2002) investigated $U^{VI}O_2^{2+}$, Co^{2+}, Ni^{2+}, Ca^{2+} and Am^{3+} complexation with HA in m_{NaCl} solutions by solvent extraction methods in ambient (air) atmosphere. A summary of the experimental conditions is given in Table 1. Only data within the applicability of SIT (I < 4 m) are considered in the present study. Although Cl^- is clearly a more relevant background anion than ClO_4^- in the environment, the interpretation of M-HA complexation data obtained for high m_{NaCl} are more difficult because, unlike ClO_4^-, Cl^- is a complexing anion, albeit, a weak one. In addition, the Am- and U(VI)-HA experiments were carried out in the presence of 0.01 M acetate buffer. Acetate is known to bind to metal ions and must therefore be taken into account in the calculations (Labonne-Wall et al., 1999; Wall et al., 2002). Finally, unlike the other cations, for $pH_m \approx 5$ under ambient (air) atmosphere, UO_2^{2+} hydrolysis and complexation by carbonate anions cannot be neglected (Langmuir, 1978; Labonne-Wall et al., 1999). Therefore, M-HA complexation datasets obtained for high m_{NaCl} are less suitable for testing the applicability of NICA-Donnan and Model VII than experiments conducted in a more inert background electrolyte such as $NaClO_4$. Indeed, it was found that the modeling results discussed below strongly depend on the thermodynamic databases in solution and their respective capabilities to accurately handle the speciation of Am^{3+}, UO_2^{2+}, Ni^{2+}, Co^{2+} and Ca^{2+} in saline solutions, even in the absence of HA.

Table 1. Summary of the experimental conditions for the M-HA complexation experiments of Wall et al. (2002) (Am^{3+}), Labonne-Wall et al. (1999) (UO_2^{2+}), Kurk and Choppin (2000) (Co^{2+} and Ni^{2+}) and Laszak and Choppin (2001) (Ca^{2+}).

	[M] (mol L^{-1})	[HA] (mg L^{-1})	m_{NaCl} (m)	pH	pH buffer
Am^{3+}	1×10^{-9}	1 - 10	0.1 - 6	5.1 (pH_m)	10^{-2} M acetate
UO_2^{2+}	5.24×10^{-7}	2 - 10	0.1 - 6	4.9 (pH_m)	10^{-2} M acetate
Ni^{2+}	1×10^{-9}	2×10^{-3} - 1.6×10^{-2}	0.3 - 5	6.0 (pH_{exp})	No
Co^{2+}	1×10^{-10}	1.3×10^{-2} - 2.2×10^{-1}	0.3 - 5	6.0 (pH_{exp})	No
Ca^{2+}	1×10^{-8}	0 - 500	0.1 - 3	4.5 - 9.5 (pH_m)	No

The reported M-HA complexation constants pertain to the PM (Labonne-Wall et al., 1999; Kurk and Choppin, 2000; Laszak and Choppin, 2001; Wall et al., 2002). For the studies listed in Table 1, α_{HA} values were determined for each pH and *I* from HA proton titrations for the specific metal ion-HA complexation studies. Because NICA-Donnan and Model VII are able to describe M-HA complexation as a function of the pH, it is more convenient to compare experimental constants that have not been corrected for α_{HA}. This can be easily accomplished because all of these studies focused on low metal loadings, where [MHA] can be neglected in eq. 6 (i.e., $[HA]_f \approx [HA]_{tot} \times \alpha_{HA}$). Note that the carboxylic groups of HA were considered responsible for M-HA complexation and only these groups were considered in the calculation of $[HA]_{tot}$ (eq. 5-6) (Labonne-Wall et al., 1999; Laszak and Choppin, 2001; Wall et al., 2002). Labonne-Wall et al. (1999) and Wall et al. (2002) reported 1:1 and 1:2 UO_2^{2+}/Am^{3+}-HA complexation constants. Because, the constants show similar variation with *I*, either for UO_2^{2+} or Am^{3+}, the 1:2 complexes are not discussed here and the simulations are made for the lowest [HA] investigated experimentally (i.e., where the 1:1 complex prevails).

Am(III). Wall et al. (2002) investigated the effect of NaCl on Am-HA complexation for pH_m = 5.1 in 0.01 M acetate buffer. Although constants were corrected for effects of side

reactions, such as the formation of Am^{3+}-acetate complexes (eq. 4), Am-Cl complexation was not taken into account by the original authors. Side reaction corrections for the formation of Am^{3+}-acetate complexes employed stability constants reported by Moore et al. (1999).

Our simulations using Model VII and NICA-Donnan are for the lowest HA concentration ([HA] = 1 mg L^{-1}). Preliminary calculations showed that Am-Cl and Am-acetate complexation have no more than a minor impact on the trend in ${}^{HA}K(Am^{3+})$ versus *I*. Experimental and simulated results (now accounting for Am-Cl complexation) are compared on Figure S5. Good prediction of Am^{3+}-HA binding is obtained by both models using generic parameters for $I = 0.1$ m, where experimental uncertainty is relatively large, whereas data for all other *I* are overestimated (see Fig. S5). To better compare experimental and simulated effects of *I* on ${}^{HA}K(Am^{3+})$, model results were decreased by 1.5 log unit on Figure 4a. In fact, the adjustment of Am-HA binding parameters would produce the same results. When using the generic Am-HA binding parameters, both models produce similar results, especially for the evolution of log K with *I*, as would be expected from the similar variation of Ψ_0 and Ψ_D with *I* (Fig. 1a). Although model log ${}^{HA}K(Am^{3+})$ values variations with *I* are not as pronounced as experimental ones, the trend is consistent. Nearly constant log ${}^{HA}K(Am^{3+})$ values are predicted for $I > 1$ *m* by both approaches, which agrees relatively well with the experimental results. Unlike Model VII (where $\Psi_0 = 0$ for $I > 1$ *m*), NICA-Donnan predicts a slight decrease of ${}^{HA}K(Am^{3+})$ for $I > 1$ *m*. This is related to the evolution of Ψ_D with *I*, and the fact that NICA-Donnan equations do not account for $\gamma_{Am^{3+}}$. Overall, the deviation between both models is small, as expected (Fig. 1a), showing that, by accounting for electrostatic effects, results from Model VII and NICA-Donnan can be extrapolated to highly saline conditions, provided that the specific binding parameters are calibrated for the respective type of HA.

U(VI). Labonne-Wall et al. (1999) investigated the effect of *I* on U(VI)-HA complexation for pH_m = 4.9 and 0.01 M acetate. UO_2^{2+}-acetate complexation constants were taken from Moore et al. (1999) and are also presently used. We simulated the experimental data of Labonne-Wall et al. (1999) using Model VII and NICA-Donnan for the lowest HA concentration ([HA] = 2 mg L^{-1}) and the generic U(VI)-HA binding parameters. As for Am, preliminary tests showed that inclusion or omission of UO_2^{2+}-Cl complexation did not impact the trend in ${}^{HA}K(UO_2^{2+})$ versus *I*. Experimental and simulated results are compared on Figure 4a. The generic U(VI)-HA parameters produce accurate predictions of the ${}^{HA}K(UO_2^{2+})$ measured by Labonne-Wall et al. (1999) as well as the evolution of ${}^{HA}K(UO_2^{2+})$ with *I* up to 2 *m*. At *I* = 3 m, a higher ${}^{HA}K(UO_2^{2+})$ value than at *I* = 2 *m* was measured, which is also predicted by Model VII. As in the case of Pu^{4+}, where the apparent hydrolysis constants increase with m_{NaClO_4} above 1 m, this increase in ${}^{HA}K(UO_2^{2+})$ is driven by $\alpha_{U(VI)}$. Similar conclusions can be made with NICA-Donnan, except a smaller re-increase in ${}^{HA}K(UO_2^{2+})$ that was observed with increasing *I*, as seen and explained for Am^{3+}. Interestingly, in agreement with the experimental data, Model VII and NICA-Donnan predict a more pronounced decrease in ${}^{HA}K(Am^{3+})$ than for ${}^{HA}K(UO_2^{2+})$ when *I* increases from 0 to 1 *m*. This feature is driven by the Boltzman factor (eq. 9), which involves the net charge of the cation (i.e. +3 versus +2, respectively) for Am(III) and U(VI).

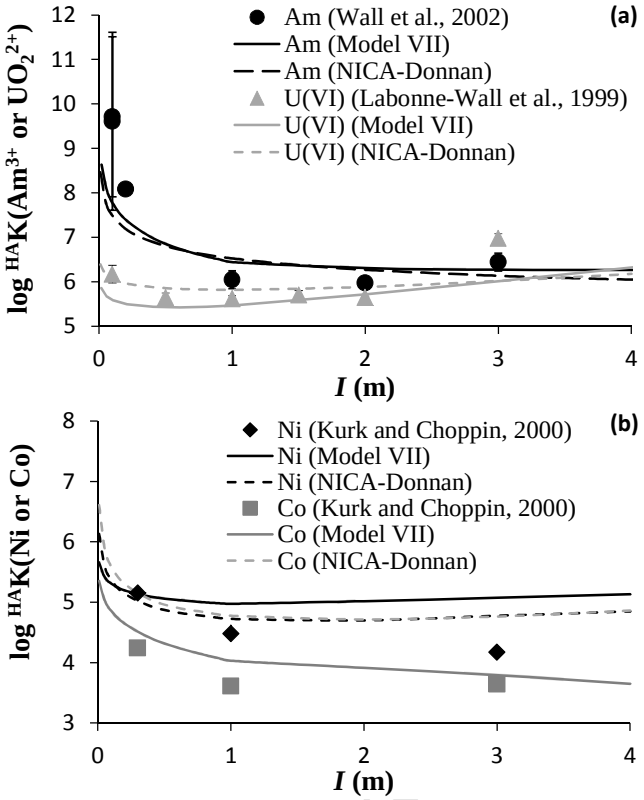

Figure 4. (a) Apparent Am-HA and U(VI)-HA complexation constants (Wall et al., 2002; Labonne-Wall et al., 1999) versus *I* (NaCl) for pH_m = 5.1 and 4.9, respectively. (b) Apparent M-HA complexation constants (M = Ni^{2+} or Co^{2+}, Kurk and Choppin, 2000) versus *I* (NaCl) for pH_{exp} = 6. For both figures, lines are predictions by Model VII (full line) and NICA-Donnan (dashed lines) using the generic parameters (but shifted down for the case of Am-HA, see text for details). Experimental error bars are commonly smaller than the symbols.

Co(II)/Ni(II). Kurk and Choppin (2000) investigated the effect of *I* on Co- and Ni-HA complexation. Unlike Am and U(VI), with data obtained for constant pH_m, Co and Ni data are reported for constant pH_{exp} = 6 by Kurk and Choppin (2000), noting that the deviation between pH_{exp} and pH_m increases with increasing *I*. For example, for pH_{exp} = 6 and *I* = 4 *m*, and with the calibration provided by the original authors, the corresponding pH_m value is 6.95. The originally reported constants were not corrected for side reactions. Again, our simulations using Model VII

and NICA-Donnan were conducted using the lowest HA concentrations reported by Kurk and Choppin (i.e., [HA] = 1.3×10^{-2} mg L^{-1} for Co; [HA] = 2×10^{-3} mg L^{-1} for Ni).

Experimental and simulated results are compared on Figure 4b. With the generic Co/Ni-HA parameters, Model VII overestimates Co/Ni-HA complexation by 1 log unit in the worst case (i.e., for $^{HA}K(Ni)$ at I = 3 m). Model VII consistently predicts a decrease in ^{HA}K with I increasing from 0.3 to 1 m, whereas for I > 1 m, the predicted ^{HA}K for Co and Ni diverge. Although pH_m increases by 0.6 units (for constant pH_{exp}) between I = 1 and 3 m, $^{HA}K(Ni)$ remains almost constant, whereas $^{HA}K(Co)$ decreases by 0.2 log units. These variations reflect the complexation of both of these transition metals by Cl^- in solution. In the SIT database provided with PHREEQC, only the $NiCl^+$ species is included, with $\varepsilon(NiCl^+;Cl^-)$ = 0.1, whereas four Co-Cl complexes are considered (i.e., from $CoCl^+$ to $CoCl_4^{2-}$), all without SIT parameters (i.e. $\varepsilon(i;k)$ = 0). In the SIT database provided with Visual MINTEQ, Co- and Ni-Cl complexation are described similarly and NICA-Donnan predicts the same trend in $^{HA}K(Ni)$ and $^{HA}K(Co)$ versus I. The reliability of the thermodynamic aqueous databases is beyond the scope of the present paper. Nonetheless, despite the potential uncertainties in the databases, overall, the predicted effect of I is relatively small above 1 m for both Ni and Co, in agreement with the experimental results.

Ca(II). Figure 5 shows $^{HA}K(Ca^{2+})$ measured by Laszak and Choppin (2001) for m_{NaCl} = 0.1, 1 and 3 m at various pH_m under ambient atmosphere. The originally reported constants were corrected for side reactions (including Ca complexation to chloride and carbonate). Simulations are made with Model VII and NICA-Donnan for 100 mg L^{-1} HA using the generic Ca-HA binding parameters and compared to experimental log $^{HA}K(Ca^{2+})$ versus pH_m for I = 0.1 and 3 m (NaCl) in Figure 5. Simulations with Model VII for I = 1 m do not significantly differ from I = 3 m and consequently are not shown. Experimentally, $^{HA}K(Ca^{2+})$ increases with pH_m and decreases with increasing I, as for the other cations investigated. Both Model VII (Fig. 5a) and NICA-

Donnan do a relatively good job at predicting these trends, although the measured effect of *I* is weaker between 0.1 and 1 *m*, and log $^{HA}K(Ca^{2+})$ are not predicted to evolve substantially for *I* between 1 and 3 *m* with Model VII. Interestingly, the measured effect of *I* appears more pronounced for $pH_m \approx 9$ than for $pH_m \approx 6.5$, which is indeed predicted by both models as anticipated (eq.16). According to the models, the larger negative charge of HA (*Q* being proportional to Ψ_0 *or* Ψ_D) at high pH is responsible for the larger ionic strength dependence of $^{HA}K(Ca^{2+})$.

To summarize, beside the deviations between experimental and simulated results that are directly related to the parameterization of $Am^{3+}/UO_2^{2+}/Co^{2+}/Ni^{2+}/Ca^{2+}$-HA complexation for a specific type of HA, the generally observed log $^{HA}K(M^{z+})$ dependence with *I* is relatively well predicted at low metal ion concentration by simply suppressing the electrostatic term in Model VII for $I > 1$ *m*. The NICA-Donnan model shows very similar results without the need to modify the model. More experimental results are required, however, to parameterize these models at high *I* and to test the relevance of additional corrections at high *I* to explain the noted discrepancies, which would make the models more complex. More specifically, complexation studies in non-complexing background electrolyte (e.g., $NaClO_4$) in the absence of pH-buffer (e.g., without acetate) and under inert atmosphere (i.e., in the absence of carbonate) are recommended.

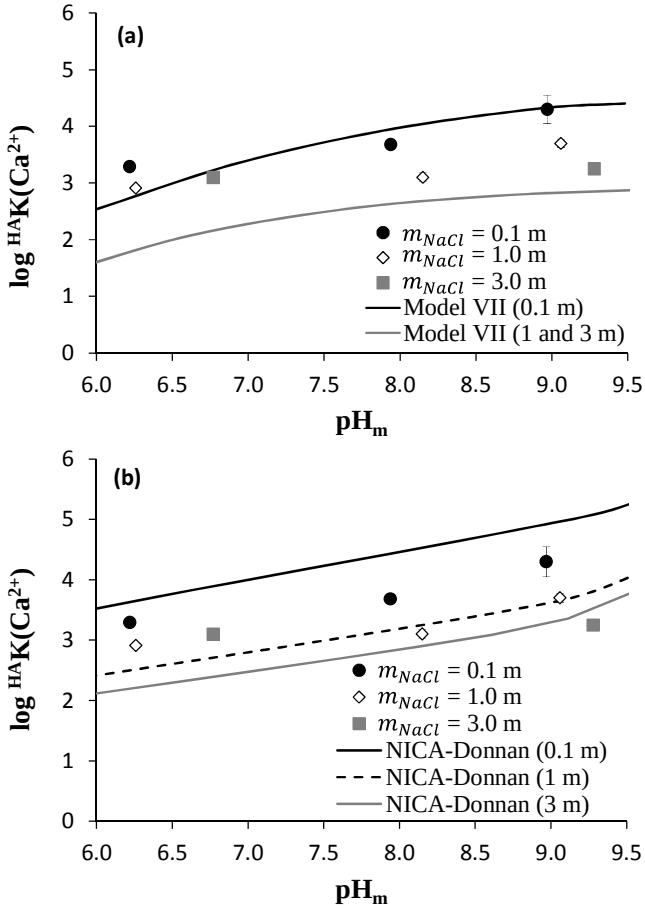

Figure 5. Experimental apparent Ca^{2+}-HA complexation constants versus pH_m for I = 0.1, 1 and 3 m NaCl (Laszak and Choppin, 2001) compared with (a) Model VII (simulated curves for I = 1 and 3 m NaCl overlap) and (b) NICA-Donnan predictions. Experimental error bars are commonly smaller than the symbols on all three figures.

3.5. Metal ion-HA complexation using SIT

To apply simple models such as the PM or the CNM to various ionic strength solutions, they must include the activities of the aqueous species. According to equations 1 and 3, when all physico-chemical conditions are kept constant except I (pH, T, total metal ion concentration), the value of log β (i.e. log ^{HA}K, log $^{HA}\beta_{\alpha}$, or log $^{HA}\beta_{LC}$) can be extrapolated to I = 0 (log β_0) using:

$$\log \beta = \log \beta_0 - \Delta z^2 \times D - \Delta \varepsilon \times I. \quad (17)$$

For 1:1 complexes between a metal ion (M^z) and a simple ligand (L^y), $\Delta\varepsilon = \varepsilon(ML^{y+z},k) - \varepsilon(M^z,k) - \varepsilon(L^y,k)$, and $\Delta z^2 = (z+y)^2 - z^2 - y^2$. Due to the complexity of HA, Δz^2 and $\Delta\varepsilon$ become adjustable parameters of unclear physical meaning (Czerwinski et al., 1996; Szabò et al., 2010).

Comparing Fig. 2b and Fig. 4a, the effect of *I* on Am-HA complexation appears to differ between the studies of Wall et al. (2002) and Czerwinski et al. (1996), but it is difficult to directly compare the original datasets because: (i) the thermodynamic constants refer to different models; (ii) pH_m differs by one unit; and (iii) the metal loading differs by 3 orders of magnitude. As in Figure 4a for the log ${}^{HA}K$ values reported by Wall et al. (2002), log ${}^{HA}\beta_{LC}$ values determined by Czerwinski et al. (1996) are recalculated to log ${}^{HA}K$ values using the *LC* values and imposing negligible [AmHA] in eq. 8. The results are shown in Figure 6a. Although Wall et al. (2002) studied Am-HA complexation at one pH_m unit lower than Czerwinski et al. (1996), their log ${}^{HA}K$ values are higher. This can be attributed to the effect of the metal loading. Specifically, at low loading, Am binds to low abundance, strong HA sites, whereas, at high loading, these sites are saturated and Am mainly binds to the more abundant, weaker HA sites (e.g., see Marsac et al., 2010). The effect of *I* below 1 *m* is more pronounced for the dataset of Wall et al. (2002), which would lead to different SIT parameters (Δz^2 and $\Delta\varepsilon$) in eq. 17. Therefore, it is difficult to confidently apply an ionic strength correction for cation-HA binding constants using simple metal ion-HA binding models.

The different ionic strength effects observed by Wall et al. (2002) and Czerwinski et al. (1996) might also arise from differences in metal loading. As pointed out by Hummel et al. (2000), ionic strength effects tend to vanish at high loadings. To illustrate this, log ${}^{HA}K$ values for Am-HA complexation are calculated using both Model VII and NICA-Donnan for pH = 5.5, $10^{-3} < I < 4$ *m* (NaCl), 1 mg L^{-1} HA, and $[Am]_{tot} = 10^{-9}$ or 10^{-6} m. The results are normalized to the log

^{HA}K value obtained for I = 1 m (i.e. log ^{HA}K(I) – log ^{HA}K(I = 1 m)) and plotted versus I in Figure 6b. Both models indeed predict a more pronounced effect of I on log ^{HA}K at low loading.

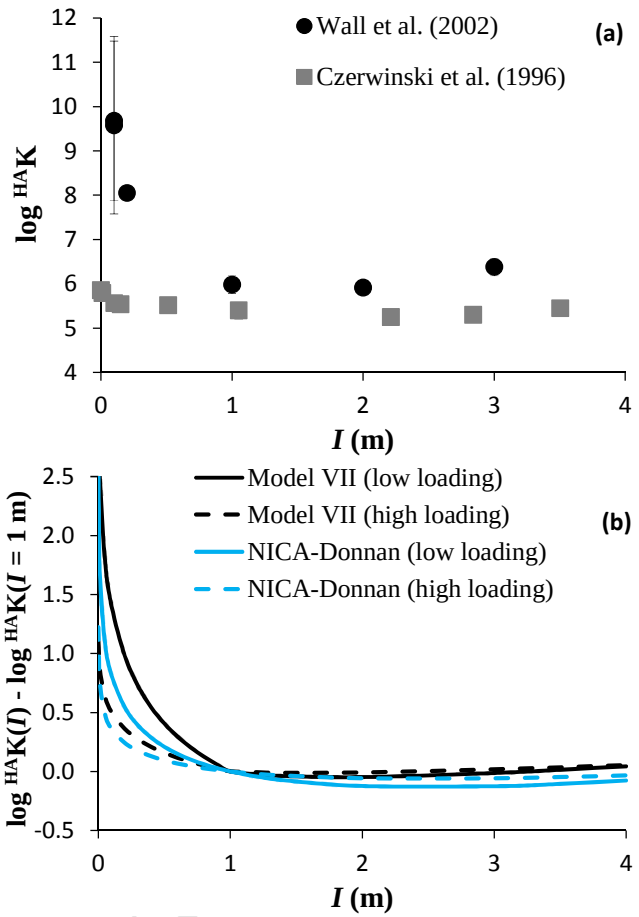

Figure 6. (a) Experimentally observed effect of the ionic strength on Am-HA complexation at low (Wall et al., 2002; pH_m = 5.1; NaCl) and high metal loading (Czerwinski et al., 1996; pH_m = 6; $NaClO_4$). (b) Simulated effect of the ionic strength on Am-HA complexation at low ($[Am]_{tot}$ = 10^{-9} m) and high metal loading ($[Am]_{tot}$ = 10^{-6} m) with Model VII (black curves) and NICA-Donnan (blue curves) in NaCl for a HA concentration of 1 mg L^{-1} and pH = 5.5. (For interpretation to references to color, the reader is referred to the web version of this article.)

The effect of I on cation-HA complexation is commonly discussed in terms of conformational changes, which make the physical meaning of the values of SIT parameters in the case of humic materials questionable. Multivalent ions are known to bridge between organic

molecules (Kunhi Mouvenchery et al., 2012), and high concentrations of trivalent actinides lead to the aggregation of HA (Lippold et al., 2005). Hence, the different evolution of log ^{HA}K with *I* observed by Wall et al. (2002) and Czerwinski et al. (1996) may be partially attributed to the aggregation state (or the conformation) of HA in response to different [Am] to [HA] ratios. In Model VII, conformational changes of HA in response to variations of *I* are not explicitly treated, except via a change in Donnan volume, which we find to have a negligible effect on M-HA complexation in saline solutions. Because the charging behavior of HA is related to its conformation, such behavior can implicitly be taken into account within the electrostatic term. In NICA-Donnan, the ionic strength directly affects the Donnan volume. However, none of these models includes effects of conformational changes of HA when $[Am]_{tot}$ increases (e.g., in the case of NICA-Donnan, 10^{-6} *m* of Am would not affect the Donnan volume), by contrast with the more recent Elastic Polyelectrolyte Network electrostatic model (Montenegro et al., 2014). Instead, NICA-Donnan and Model VII explain the less pronounced effect of *I* at increased loading via the charging behavior of HA. In the experiments of Czerwinski et al. (1996), the observed *LC* ranges between 50 and 70% of the PEC. The charge of HA is almost neutralized by Am at the highest $[Am]_{tot}$ investigated, which decreases electrostatic effects and flattens the log ^{HA}K versus *I* curve. Therefore, metal loading is an important parameter not only for the determination of apparent metal ion-HA complexation constants for given pH and *I* conditions, but also for their extrapolation to various ionic strengths (e.g., with SIT).

Unlike Na, with non-specific HA interaction, Ca and Mg bind more strongly to HA, and consequently may affect the charge of HA in brines. Furthermore, other metal ions (e.g. Fe(III), Al(III), divalent transition metals) strongly bind to HA in natural conditions (Kinniburgh et al., 1999; Pinheiro et al., 2000; Tipping et al., 2002; Gustafsson et al., 2007; Marsac et al., 2012; 2013). Hence, the metal loading must be defined on the basis of all cations bound to HA,

including H^+. Additional cation competition studies should be conducted at high *I* to improve and homogenize metal ion-HA binding models. As an example, in NICA-Donnan Ca^{2+} mainly interacts electrostatically with HA at high [Ca^{2+}] (Christl, 2012) whereas it chiefly binds specifically to HA in Model VII. As shown in Figure S6, Model VII predicts larger effects from [Ca] on Am-HA complexation than does NICA-Donnan. For pH = 5, 1 m NaCl, [Am] = 10^{-9} m and 1 mg L^{-1} HA, between 0 and 1 m $CaCl_2$, Model VII predicts a decrease of ${}^{HA}K(Am)$ by 1.5 log units against 0.9 using NICA-Donnan. These results highlight another source of variation and uncertainty for Δz^2 and $\Delta\varepsilon$ at high [Ca]. Because it is also suggested that Ca^{2+}-HA interaction is purely electrostatic (van Leeuwen and Town, 2016), Ca^{2+}-metal ion competition experiments at high *I* are required to unravel the role of Ca on metal ion-HA complexation.

As shown above, the ionic strength dependence of ${}^{HA}K(Ca^{2+})$ becomes more pronounced at high pH because of the higher charge of HA. It appears that Δz^2 and $\Delta\varepsilon$, when applied to simple models for M-HA complexation, remain conditional parameters, which depend on the pH, the ionic strength, and the composition of the solution, which in turn affects the loading of HA. Therefore, empirical determination of Δz^2 and $\Delta\varepsilon$ for various conditions requires a large experimental dataset. Because most metal ion-HA binding data at $I > 1$ m were obtained at $pH_m \leq 6$, data at higher pH would be necessary to further test the reliability of NICA-Donnan and Model VII.

More generally, the use of non-electrostatic models was recently shown to be particularly suitable for the prediction of metal ion sorption to various types of surfaces in brines, including marine microalgae (Schjif and Herbling, 2010; Zoll and Schjif, 2012), bacteria (Ams et al., 2013), illite and smectite (Schnurr et al., 2015). The present data evaluation suggests that this approach can be extended to humic substances using Model VII. Although NICA-Donnan

remains an electrostatic model in highly saline solution, the almost invariant Donnan potential produces similar ionic strength effects to those observed using Model VII.

4. Conclusions

The applicability of Model VII and NICA-Donnan was tested at high 1:1 background electrolyte concentration ($NaCl/ClO_4$) in combination with SIT (I < 4 m). The empirical electrostatic term used in Model VII is related to the constant capacitance model (CCM). A method is proposed to use the CCM in the speciation code PHREEQC, for easier and more consistent implementation of Model VII in this code. The electrostatic term used in this model tends towards zero for I = 1 m, and thus, further metal ion accumulation in the vicinity of HA molecules can be neglected. Consequently, a non-electrostatic model in combination with the binding site definition in Model VII was tested for I > 1 m. The approach simplifies the model under these high ionic strength conditions, whereas NICA-Donnan can be used without modification. Both models do a relatively good job in predicting proton dissociation for HA groups where the apparent pK_a variations at high I are mainly controlled by the activity coefficient of the proton. The trend in apparent metal ion-HA complexation constants with I is consistent with experimental results for Am^{3+}, UO_2^{2+}, Co^{2+}, Ni^{2+}, Ca^{2+} and Pu^{4+}, both at low and high metal loading. The maximum metal ion uptake by HA (e.g., the loading capacity) for various conditions is relatively well predicted. Because of the simple approaches used here and due to the limited number of datasets that are available for highly saline solutions, no attempt was made to improve the models in order to eliminate the discrepancies observed in the evolution of apparent complexation constants with I. Most of the discrepancies between experiments and predictions with Model VII or NICA-Donnan are related to the specific cation-HA binding parameters used. With appropriately calibrated specific binding parameters for a given type of HA (e.g. a given composition or origin), both models are expected to reliably predict cation-HA binding for a wide range of ionic strengths.

The impact of the physico-chemical conditions on the experimental determination of SIT parameters for metal ion-HA complexation was also discussed. When HA is treated as a simple dissolved ligand, the obtained SIT parameters values are difficult to interpret with regards to their specific physical meaning owing to the complexity of HA molecules. It is shown here that the experimentally investigated pH and metal loading variations have a strong impact on SIT parameters via their effect on the charge of HA. Some effects of pH and metal loading on cation-HA complexation are well known, but the present study shows that they imply additional effects related to HA charge, which must be taken into account when extrapolating constants at various ionic strengths. Unlike Na, which only interacts electrostatically with HA, Ca or Mg can bind more strongly to HA. Because, highly saline waters commonly have substantial Ca or Mg concentrations, as well as other metal ions, relatively high overall loadings are to be expected. Although Model VII and NICA-Donnan can account for both the metal loading effects and cation competition at $I < 1$ m, additional cation competition experiments at high ionic strength are required to further validate or improve these models. Nevertheless, we suggest that both models might be used as helpful predictive tools in performance safety assessment even under highly saline conditions.

Aknowledgements

This work was financed by the Federal Ministry of Economic Affairs and Energy (Germany) under contracts No. 02E10206 and 02E10961. K. H. Johannesson thanks Michael and Mathilda Cochran for establishing the Cochran Family Professorship in Earth and Environmental Sciences, which provided her financial assistance. We thank three anonymous reviewers and the associate editor (J. P. Gustafsfson) for interesting comments that substantially improved this manuscript.

References

Altmaier M., Metz V., Neck V., Müller R. and Fanghänel Th. (2003) Solid-liquid equilibria of $Mg(OH)_{2(cr)}$ and $Mg_2(OH)_3Cl{\bullet}4H_2O_{(cr)}$ in the system Mg-Na-H-OH-Cl-H_2O at 25 °C. Geochim. Cosmochim. Acta 67, 3595-3601.

Ams D. A., Swanson J. S., Szymanowski J. E. S., Fein J. B., Richmann M. and Reed D. T. (2013) The effect of high ionic strength on neptunium (V) adsorption to a halophilic bacterium. Geochim. Cosmochim. Acta 110, 45-57.

Appelo C. and Postma D. (2005) Geochemistry, groundwater and pollution. second ed. Taylor & Francis, New York, p. 595.

Benedetti M. F., Milne C. J., Kinniburgh D. G., van Riemsdijk W. H. and Koopal L. K. (1995) Metal-ion binding to humic substances: application of the nonideal competitive adsorption model. Environ. Sci. Technol. 29, 446–457.

Benedetti M. F., van Riemsdijk W. H. and Koopal L. K. (1996) Humic substances considered as a heterogeneous Donnan gel phase. Environ. Sci. Technol. 30, 1805-1813.

Catrouillet C., Davranche M., Dia A., Bouhnik-Le Coz M., Marsac R., Pourret O. and Gruau G. (2014) Geochemical modeling of Fe(II) binding to humic and fulvic acids. Chem. Geol. 372, 109-118.

Catrouillet C., Davranche M., Dia A., Bouhnik-Le Coz M., Pédrot M., Marsac R. and Gruau G. (2015) Thiol groups controls on arsenite binding by organic matter: New experimental and modeling evidence. J. Coll. Int. Sci. 460, 310–320.

Ciavatta, L. (1980). The specific interaction theory in the evaluating ionic equilibria. Ann. Chim. (Rome) 70, 551–562.

Christl I. (2012) Ionic strength- and pH-dependence of calcium binding by terrestrial humic acids. Environ. Chem., 9, 89-96.

Czerwinski K. R., Kim J. I., Rhee D. S. and Buckau G. (1996) Complexation of trivalent actinide ions (Am^{3+}, Cm^{3+}) with humic acid: the effect of ionic strength. Radiochim. Acta 72(4), 179-187.

Fritz P. and Frape S. K. (1982). Saline Groundwaters in the Canadian shield – a first overview. Chem. Geol. 36, 179-190.

Grenthe I., Plyasunov A. V. and Spahiu K. (1997) Estimations of Medium Effects on Thermodynamic Data. Chapter IX in “Modeling in aquatic chemistry”. OECD Publications, 724 pp. ISBN 92-64-15569-4.

Guillaumont R., Fanghänel Th., Fuger J., Grenthe I., Neck V., Palmer D. A. and Rand M. H. (2003) Update on the Chemical Thermodynamics of Uranium, Neptunium, Plutonium, Americium and Technetium, Mompean, F.J., Domenech-Orti, C., Ben-Said, K., OECD/NEA Data Bank, Eds., vol. 5 of Chemical Thermodynamics, Elsevier, Amsterdam.

Gustafsson J. P. Visual MINTEQ version 3.0. http://vminteq.lwr.kth.se/. Stockholm, Sweden, Octobed 2012.

Gustafsson J. P., Persson I., Kleja D. B. and van Schaik J. W. J. (2007) Binding of iron(III) to organic soils: EXAFS spectroscopy and chemical equilibrium modeling. Environ. Sci. Technol. 41, 1232-1237.

Hesterberg D., Chou J. W., Hutchison K. J. and Sayers D. E. (2001) Bonding of Hg(II) to reduced organic, sulfur in humic acid as affected by S/Hg ratio. Environ. Sci. Technol. 35, 2741–2745.

Hiemstra T. and van Riemsdijk W. (2006) Biogeochemical speciation of Fe in ocean water. Mar. Chem. 102, 181–197.

Hummel W., Glaus M. A. and Van Loon L. R. (2000) Trace metal-humate interactions. II. The "conservative roof" model and its application. Appl. Geochem. 15, 975-1001.

Kim J. I. and Czerwinski K. R. (1996) Complexation of metal ions with humic acid: metal ion charge neutralisation model. Radiochim. Acta 73, 5–10.

Kinniburgh D. G., Milne C. J., Benedetti M. F., Pinheiro J. P., Filius J., Koopal L. and Van Riemsdijk W. H. (1996) Metal ion binding by humic acid: application of the NICA-Donnan model. Environ. Sci. Technol. 30, 1687–1698.

Kinniburgh D. G., van Riemsdijk W. H., Koopal L. K., Borkovec M., Benedetti M. F. and Avena M. J. (1999) Ion binding to natural organic matter: competition, heterogeneity, stoichiometry and thermodynamic consistency. Colloid Surf. A 151, 147-166.

Koopal L. K., Saito T., Pinheiro J. P. and van Riemsdijk W.H. (2005) Ion binding to natural organic matter: General considerations and the NICA–Donnan model. Colloids and Surfaces A: Physicochem. Eng. Aspects 265, 40–54.

Kunhi Mouvenchery Y., Kučerík J., Diehl D. and Schaumann G. E. (2012) Cation-mediated cross-linking in natural organic matter: a review. Rev. Environ. Sci. Biotechnol. 11, 41–54.

Kurk D. N. and Choppin G. R. (2000) Determination of Co(II) and Ni(II)-humate stability constants at high ionic strength NaCl solutions. Radiochim. Acta 88, 583–586.

Langmuir D. (1978) Uranium solution-mineral equilibria at low temperatures with applications to sedimentary ore deposits. Geochim. Cosmochim. Acta 42, 547-569.

Labonne-Wall N., Choppin G. R., Lopez C. and Monsallier J.-M. (1999) Interaction of uranyl with humic and fulvic acids at high ionic strength. In: Actinide speciation in high ionic strength media: experimental and modeling approaches to predicting actinide speciation and migration in the subsurface. Eds. Reed D. T., Clark S. B. and Rao L., Plenum Pub., NY, p. 199.

Laszak I. and Choppin G. R. (2001) Interaction study between Ca^{2+} and humic acids in brine media. Radiochim. Acta 89, 653–659.

Lippold H., Mansel A. and Kupsch H. (2005) Influence of trivalent electrolytes on the humic colloid-borne transport of contaminant metals: competition and flocculation effects. J. Cont. Hydrol. 76, 337–352.

Liu D. J., Bruggeman C. and Maes N. (2008) The influence of natural organic matter on the speciation and solubility of Eu in Boom Clay porewater. Radiochim. Acta 96, 711–720.

Lützenkirchen J. (1999) The Constant Capacitance Model and Variable Ionic Strength: An Evaluation of Possible Applications and Applicability. J. Coll. Int. Sci. 217, 8-18.

Lützenkirchen J., van Male J., Leermakers F. and Sjöberg S. (2011) Comparison of various models to describe the charge-pH dependence of poly(acrylic acid). J. Chem. Eng. Data 56, 1602-1612.

Maes A., Tits J., Mermans G. and Dierckx A. (1992) Measurement of the potentially available charge and the dissociation behaviour of humic acid from cobaltihexammine adsorption. J. Soil Sci. 43, 669-677.

Marinsky J. A., Gupta S. and Schindler P. (1982) The interaction of Cu(II) ion with humic acid. J. Coll. Int. Sci. 89, 401-411.

Marquardt C. and Kim J. I. (1998) Complexation of Np(V) with fulvic acid. Radiochm. Acta 81, 143-148.

Marsac R., Banik N. L., Marquardt C. M. and Kratz J. V. (2014) Stabilization of polynuclear plutonium(IV) species by humic acid. Geochim. Cosmochim. Acta 131, 290-300.

Marsac R., Davranche M., Gruau G. and Dia A. (2010) Metal loading effect on rare earth element binding to humic acid: Experimental and modeling evidence, Geochim. Cosmochim. Acta 74, 1749-1761.

Marsac R., Davranche M., Gruau G., Bouhnik-Le Coz M. and Dia A. (2011) An improved description of the interactions between rare earth elements and humic acids by modeling: PHREEQC-Model VI coupling. Geochim. Cosmochim. Acta 75, 5625-5637.

Marsac R., Davranche M., Gruau G., Dia A. and Bouhnik-Le Coz M. (2012) Aluminium competitive effect on rare earth elements binding to humic acid. Geochim. Cosmochim. Acta 89, 1-9.

Marsac R., Davranche M., Gruau G., Dia A., Pédrot M., Bouhnik-Le Coz M. and Briant N. (2013) Effects of Fe competition on REE binding to humic acid: Origin of REE pattern variability in organic waters. Chem. Geol. 342, 119-127.

Martell A.E. and Hancock R.D. (1996) Metal Complexes in Aqueous Solutions. New York: Kluwer.

Milne C. J., Kinniburgh D. G. and Tipping E. (2001) Generic NICA-Donnan model parameters for proton binding by humic substances. Environ. Sci. Technol. 35, 2049-2059.

Milne C. J., Kinniburgh D. G., Van Riemsdijk W. H. and Tipping E. (2003) Generic NICA-Donnan model parameters for metal-ion binding by humic substances. Environ. Sci. Technol. 37, 958–971.

Montenegro A. C., Orsetti S. and Molina F. V. (2014) Modelling proton and metal binding to humic substances with the NICA–EPN model. Environ. Chem. 11, 318-332.

Moore R. C., Borkowski M., Bronikowski M. G., Chen J.-F., Pokrovsky O. S., Xia Y. and Choppin G. R. (1999) Thermodynamic modeling of actinide complexation with acetate and lactate at high ionic strength. J. Sol. Chem. 28, 521-531.

Mühlenweg U., Brasser Th. and Hertes U. (1997) Charakterisierung von mineralisierten Tiefengrundwässern in nichtsalinaren Festgesteinen. Report GRS-144, ISBN 3-931995-04-6, Gesellschaft für Anlagen- und Reaktorsicherheit (GRS) mbH, Germany. p. 19

Parkhurst D. L. and Appelo C. A. J. (1999) User's guide to PHREEQC (Version 2) - a computer program for speciation, batch reaction, one-dimensional transport and inverse geochemical calculation. Water-resources Investigation Report 99–4259, USGS, Denver, Colorado, p. 312.

Pinheiro J. P., Mota A. M. and Benedetti M. F. (2000) Effect of aluminum competition on lead and cadmium binding to humic acids at variable ionic strength. Environ. Sci. Technol. 34, 5137-5143.

Pitzer K. S. (1991) Ion interaction approach: theory and data correlation. In: Pitzer, K.S. (Ed.), Activity Coefficients in Electrolyte Solutions. CRC Press, Boca Raton, Florida, pp. 75-153.

Rey-Castro C., Lodeiro P., Herrer R. and Sastre De Vicente M. E. (2003) Acid-base properties of brown seaweed biomass considered as a Donnan gel. A model reflecting electrostatic effects and chemical heterogeneity. Environ. Sci. Technol. 37, 5159-5167.

Ringböm A. (1963) Complexation in Analytical Chemistry. Interscience, New York.

Ritchie J. D. and Perdue E.M. (2003) Proton-binding study of standard and reference fulvic acids, humic acids, and natural organic matter. Geochim. Cosmochim. Acta 67, 85-96.

Sasaki T., Kobayashi T., Tagagi I. and Moriyama H. (2008) Discrete fragment model for complex formation of europium(III) with humic acid. J. Nucl. Sci. Technol. 45(8), 718–724.

Schijf J. and Ebling A. M. (2010) Investigation of the ionic strength dependence of Ulva lactuca acid functional group pKas by manual alkalimetric titrations. Environ. Sci. Technol. 44, 1644–1649.

Schnurr A., Marsac R., Kupcik T., Rabung T., Lützenkirchen J. and Geckeis H. (2015) Sorption of Cm(III) and Eu(III) onto clay minerals under saline conditions: Batch adsorption, Laser-fluorescence spectroscopy and modeling. Geochim. Cosmochim. Acta 151, 192-202.

Stockdale A., Tipping E., Hamilton-Taylor J. and Lofts S. (2011) Trace metals in the open oceans: speciation modelling based on humic type ligands. Environ. Chem. 8(3), 304-319.

Szabò G., Guczi J., Reiller P., Miyajima T. and Bulman R. A. (2010) Effect of ionic strength on complexation of Pu(IV) with humic acid. Radiochim. Acta 98, 13–18.

Tipping E. (1998) Humic ion-binding model VI: an improved description of the interactions of protons and metal ions with humic substances. Aquat. Geochem. 4, 3–48.

Tipping E. and Hurley M. A. (1992) A unifying model of cation binding by humic substances. Geochim. Cosmochim. Acta 56, 3627–3641.

Tipping E., Lofts S. and Sonke J. (2011) Humic ion-binding Model VII: a revised parameterisation of cation-binding by humic substances. Environ. Chem. 8, 225-235.

Tipping E., Rey-Castro C., Bryan S. E. and Hamilton-Taylor J. (2002) Al(III) and Fe(III) binding by humic substances in freshwaters and implications for trace metal speciation. Geochim. Cosmochim. Acta 66, 3211–3224

Torres R. A. and Choppin G. R. (1984) Europium(III) and Americium(III) stability constants with Humic acid. Radiochim. Acta 35(3), 143-148.

Turner A., Pedroso S. S. and Brown M. T. (2008) Influence of salinity and humic substances on the uptake of trace metals by the marine macroalga, Ulva lactuca: Experimental observations and modelling using WHAM. Mar. Chem. 110, 176–184.

van Dijk H. Z. (1959) Zur Kenntnis der Basenbindung von Huminsäuren. Pflanzenernähr. Düng. Bodenk. 84, 150-155.

van Leeuwen H. P. and Town R. M. (2016) Electric condensation of divalent counterions by humic acid nanoparticles. Environ. Chem. 13, 76-83.

Wall N. A. and Choppin G. R. (2003) Humic acids coagulation: influence of divalent cations. Appl. Geochem. 18, 1573–1582.

Wall N. A., Borkowski M., Chen J.-F. and Choppin G. R. (2002) Complexation of americium with humic, fulvic and citric acids at high ionic strength. Radiochim. Acta 90, 563–568.

Zoll A. M. and Schjif J. (2012) A surface complexation model of YREE sorption on Ulva lactuca in 0.05–5.0 M NaCl solutions. Geochim. Cosmochim. Acta 97, 183–199.

Table and figure captions:

Table 1. Summary of the experimental conditions for the M-HA complexation experiments of Wall et al. (2002) (Am^{3+}), Labonne-Wall et al. (1999) (UO_2^{2+}), Kurk and Choppin (2000) (Co^{2+} and Ni^{2+}) and Laszak and Choppin (2001) (Ca^{2+}).

Figure 1. a) Surface potential (Ψ_0) and Donnan potential (Ψ_D) calculated for Model VII and NICA-Donnan, respectively, for pH (= - log a_{H^+}) = 5.5 versus the ionic strength. The y-axis for Ψ_D is shifted by 60 mV compared with the one of Ψ_0 to highlight their similar evolution with *I*. (b) Activity coefficient of the proton ($\log \gamma_{H^+}$) versus *I* in NaCl, $NaClO_4$ and $NaNO_3$ solutions, calculated with SIT. (c) HA charge versus pH_m in 0.1 M (black curve), 1 M (blue curve), and 3 M (red curve) [0.1, 1.051, 3.503 m, respectively] $NaClO_4$. Points are experimental results of Maes et al. (1992) and lines are results from Model VII. (For interpretation to references to color, the reader is referred to the web version of this article.)

Figure 2. (a) Experimental Am-HA binding isotherms of Czerwinski et al. (1996) for pH_m = 6 and m_{NaClO_4}= 0.01, 0.1, 1 and 3.5 m (symbols) compared with simulations using Model VII (lines). Experimental (b) log ${}^{HA}\beta_{LC}$ and (c) loading capacity (*LC*) values for Am compared with Model VII and NICA-Donnan predictions versus *I* ($NaClO_4$) in the experimental conditions of Czerwinski et al. (1996). Experimental error bars are generally smaller than the symbols.

Figure 3. Experimental binding capacity (B_{max}) and log ${}^{HA}\beta(Pu^{4+})$ values of Szabò et al. (2010) versus *I* ($NaClO_4$) compared with Model VII predictions. Arrows refer to the y-axis corresponding to the data. Experimental error bars for B_{max} are generally smaller than the symbols.

Figure 4. (a) Apparent Am-HA and U(VI)-HA complexation constants (Wall et al., 2002; Labonne-Wall et al., 1999) versus *I* (NaCl) for pH_m = 5.1 and 4.9, respectively. (b) Apparent M-HA complexation constants (M = Ni^{2+} or Co^{2+}, Kurk and Choppin, 2000) versus *I* (NaCl) for pH_{exp} = 6. For both figures, lines are predictions by Model VII (full line) and NICA-Donnan (dashed lines) using the generic parameters (but shifted down for the case of Am-HA, see text for details). Experimental error bars are commonly smaller than the symbols.

Figure 5. Experimental apparent Ca^{2+}-HA complexation constants versus pH_m for I = 0.1, 1 and 3 m NaCl (Laszak and Choppin, 2001) compared with (a) Model VII (simulated curves for I = 1 and 3 m NaCl overlap) and (b) NICA-Donnan predictions. Experimental error bars are commonly smaller than the symbols on all three figures.

Figure 6. (a) Experimentally observed effect of the ionic strength on Am-HA complexation at low (Wall et al., 2002; pH_m = 5.1; NaCl) and high metal loading (Czerwinski et al., 1996; pH_m = 6; $NaClO_4$). (b) Simulated effect of the ionic strength on Am-HA complexation at low ($[Am]_{tot}$ = 10^{-9} m) and high metal loading ($[Am]_{tot}$ = 10^{-6} m) with Model VII (black curves) and NICA-Donnan (blue curves) in NaCl for a HA concentration of 1 mg L^{-1} and pH = 5.5. (For interpretation to references to color, the reader is referred to the web version of this article.)

	[M] (mol L^{-1})	[HA] (mg L^{-1})	m_{NaCl} (m)	pH	pH buffer
Am^{3+}	1×10^{-9}	1 - 10	0.1 - 6	5.1 (pH_m)	10^{-2} M acetate
UO_2^{2+}	5.24×10^{-7}	2 - 10	0.1 - 6	4.9 (pH_m)	10^{-2} M acetate
Ni^{2+}	1×10^{-9}	2×10^{-3} - 1.6×10^{-2}	0.3 - 5	6.0 (pH_{exp})	No
Co^{2+}	1×10^{-10}	1.3×10^{-2} - 2.2×10^{-1}	0.3 - 5	6.0 (pH_{exp})	No
Ca^{2+}	1×10^{-8}	0 - 500	0.1 - 3	4.5 - 9.5 (pH_m)	No

Table 1

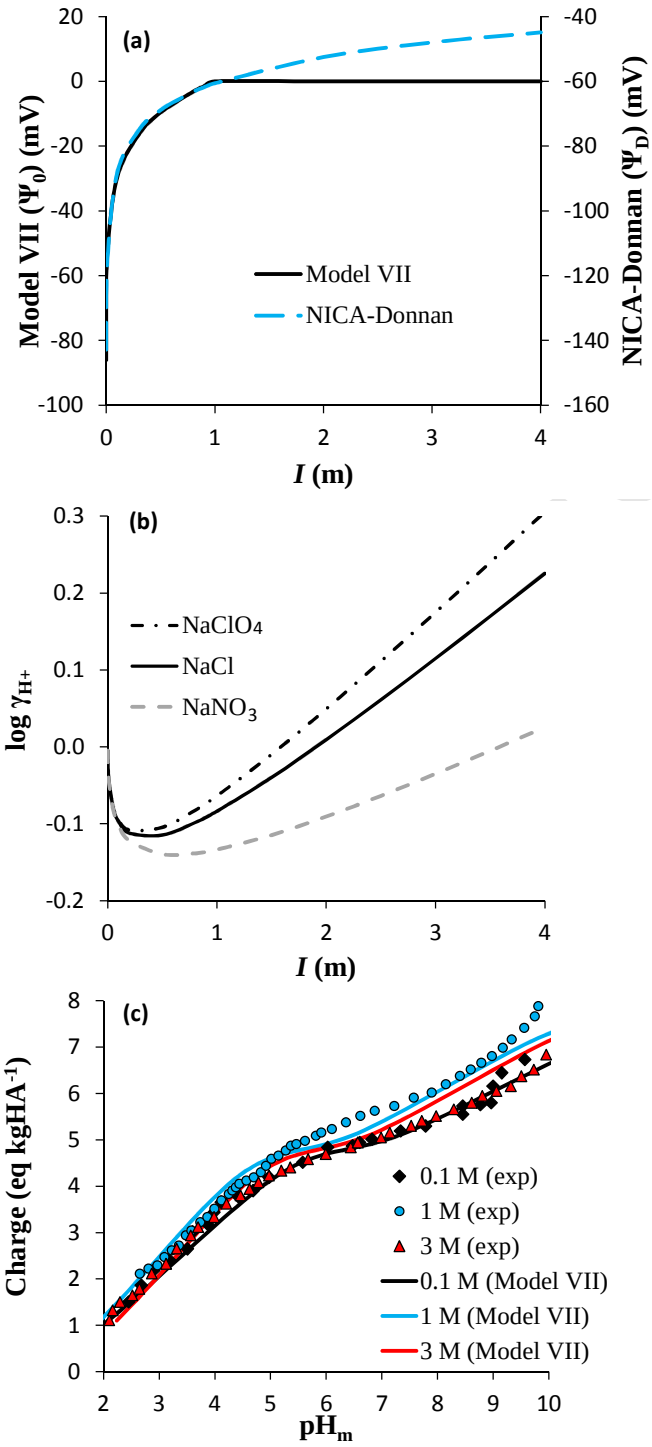
(a)
Model VII (Ψ_0) (mV)
NICA-Donnan (Ψ_D) (mV)
Model VII
NICA-Donnan
I (m)
(b)
log γ_{H+}
NaClO4
NaCl
NaNO3
I (m)
(c)
Charge (eq kgHA-1)
0.1 M (exp)
1 M (exp)
3 M (exp)
0.1 M (Model VII)
1 M (Model VII)
3 M (Model VII)
pHm

Figure 1

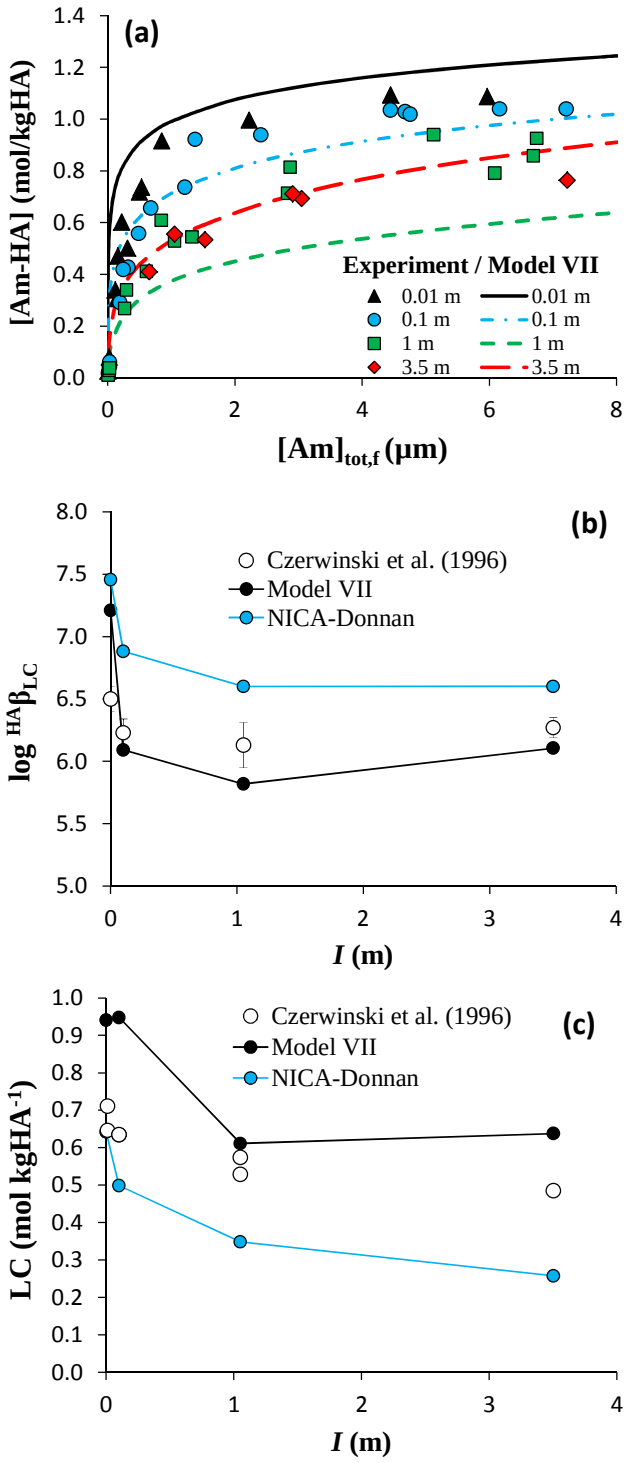
(a)
[Am-HA] (mol/kgHA)
[Am]tot,f (µm)
Experiment / Model VII
0.01 m
0.1 m
1 m
3.5 m
0.01 m
0.1 m
1 m
3.5 m
(b)
log HAβLC
I (m)
Czerwinski et al. (1996)
Model VII
NICA-Donnan
(c)
LC (mol kgHA-1)
I (m)
Czerwinski et al. (1996)
Model VII
NICA-Donnan

Figure 2

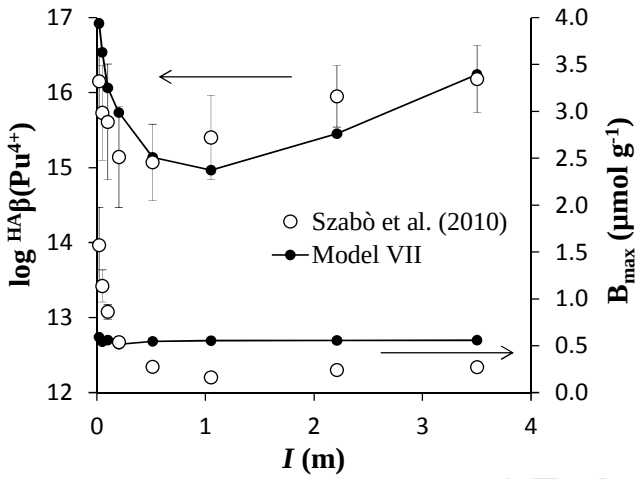

Figure 3

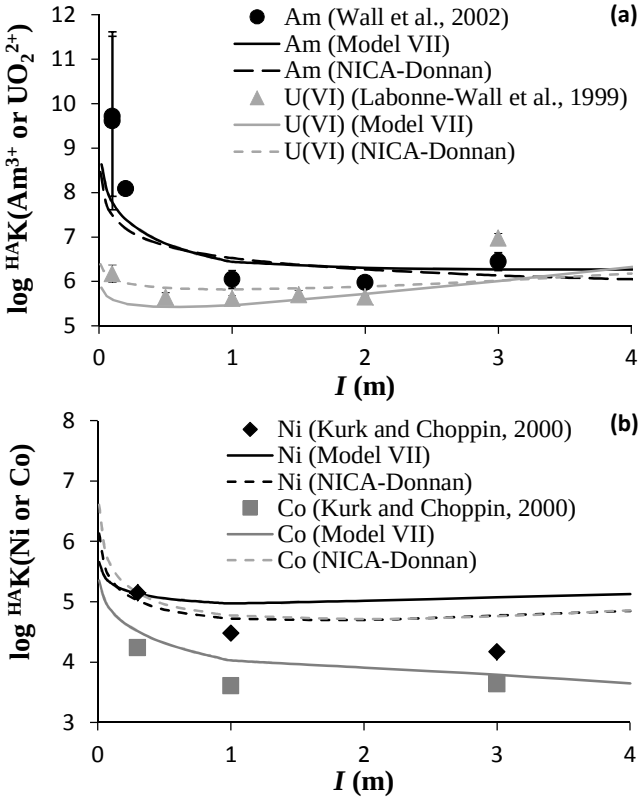

Figure 4

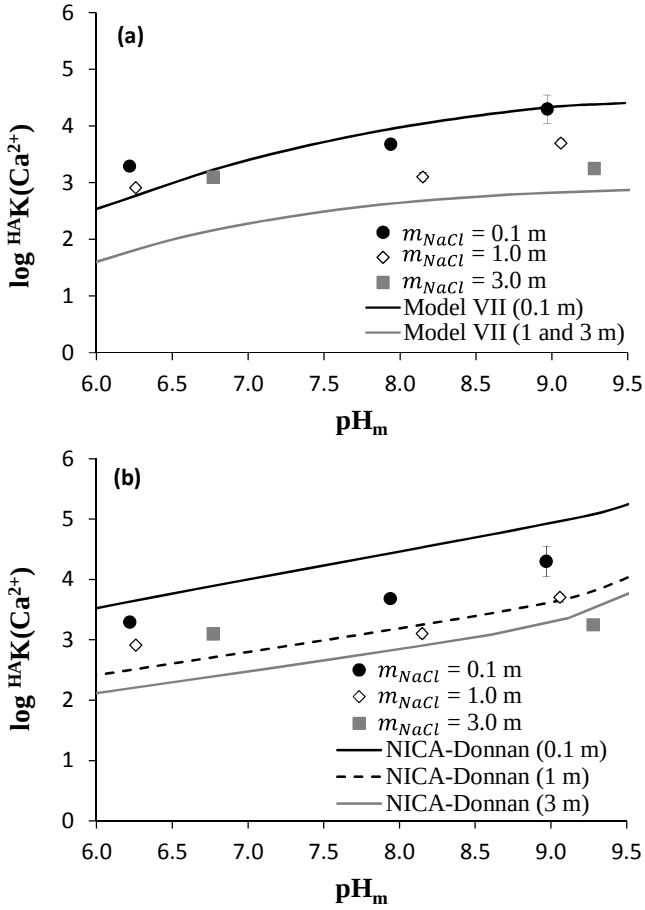
(a)
log HAK(Ca2+)
pHm
m_{NaCl} = 0.1 m
m_{NaCl} = 1.0 m
m_{NaCl} = 3.0 m
Model VII (0.1 m)
Model VII (1 and 3 m)
(b)
log HAK(Ca2+)
pHm
m_{NaCl} = 0.1 m
m_{NaCl} = 1.0 m
m_{NaCl} = 3.0 m
NICA-Donnan (0.1 m)
NICA-Donnan (1 m)
NICA-Donnan (3 m)

Figure 5

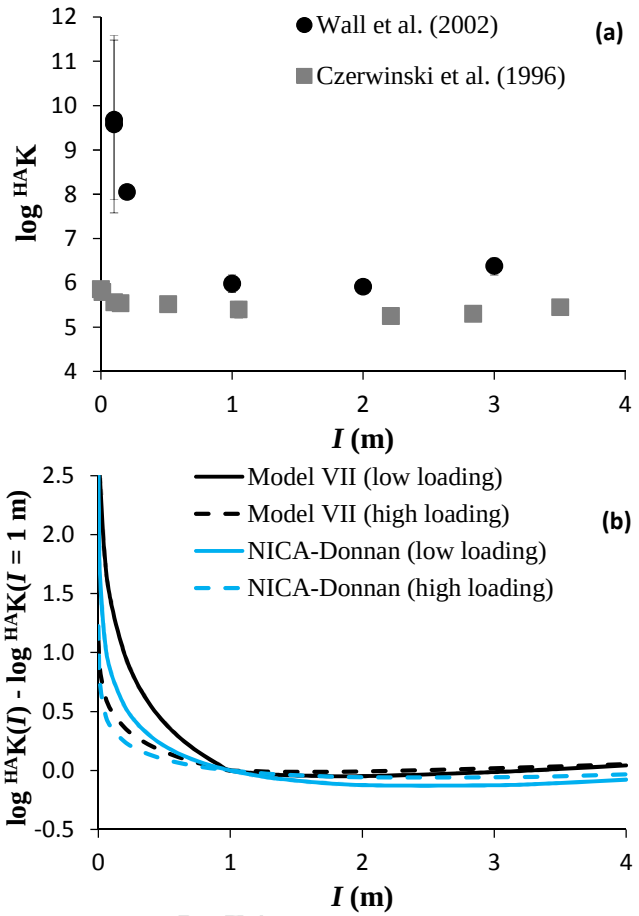
Wall et al. (2002)
Czerwinski et al. (1996)
(a)
log HAK
I (m)
Model VII (low loading)
Model VII (high loading)
NICA-Donnan (low loading)
NICA-Donnan (high loading)
(b)
log HAK(I) - log HAK(I = 1 m)
I (m)

Figure 6